Design and Clinical Evaluation of a Digital Transtibial Prosthetic Interface

by

Duncan R.C. Lee

B.S., Yale University (2020)

Submitted to the Department of Mechanical Engineering
in partial fulfillment of the requirements for the degree of

Master of Science in Mechanical Engineering

at the

MASSACHUSETTS INSTITUTE OF TECHNOLOGY

May 2022

Author .....
Department of Mechanical Engineering
May 6, 2022

Certified by .....
Hugh Herr
Professor of Media Arts & Sciences
Thesis Supervisor

Certified by .....
Amos Winter
Associate Professor, Department of Mechanical Engineering
Thesis Reader

Accepted by .....
Nicolas Hadjiconstantinou
Chairman, Committee on Graduate Students

Design and Clinical Evaluation of a Digital Transtibial Prosthetic Interface

by

Duncan R.C. Lee

Submitted to the Department of Mechanical Engineering
on May 6, 2022, in partial fulfillment of the
requirements for the degree of
Master of Science in Mechanical Engineering

Abstract

For those living with lower-limb loss, the prosthetic interface, comprising a socket and liner, is the component of the prosthesis that most limits its wearability and use. An improperly designed prosthetic interface results in excessive pressure areas that cause wear and chafing with skin breakdown as a common occurrence. Traditionally-designed interfaces require extensive time from the patient and an experienced prosthetist, with these factors compounding to make the entire process inaccessible to the majority of persons with amputation. To address these problems, this thesis outlines a prosthetic interface design and manufacturing pipeline that uses a novel computational algorithm to create subject-specific transtibial liner and socket components that can be additively manufactured at low cost. The residual limb is imaged using a magnetic resonance imaging (MRI) device, and the image set is segmented into a three-dimensional model. This approach is superior to other 3D-modeling prosthetic interface techniques as it is able to capture bone geometries and soft tissue depths of the residuum. A more accurate topology of the skin is captured using digital image correlation (DIC), and this mesh is used in replacement of the MRI skin. The socket is divided into four distinct pressure regions, and the nominal pressure applied at each region can be adjusted to be patient-specific. Finite element analysis is run to simulate liner donning and bodyweight loading upon the interface to generate the final pressure map and liner-socket geometries. Novel prosthetic interfaces made using this algorithm were evaluated against conventionally made interfaces for 5 limbs from 4 patients through a combination of kinematic gait data, standing pressure data, thermal skin measurement, and qualitative patient response. The kinematic results in this study use the Mahalanobis distance to evaluate difference in gait asymmetry resulting from conventional and novel prosthetic interfaces. The distance is calculated using asymmetries for step time, swing time, and peak impact ground reaction force. No subjects exhibit significant difference in gait asymmetry resulting from conventional and novel prosthetic interfaces (asymmetry greater than the 5% p-value was not observed for Mahalanobis distance for 3 degrees of freedom). Thermal results show no statistically significant difference in percent temperature change from reference be-

tween conventional and novel interfaces. This is true for overall temperature change as well as change at the distal and fibular head regions specifically. Further, standing pressure data do not show significant difference between conventional and novel prosthetic interfaces when the pressure variance at locations excluding the patellar bar are compared. Qualitative feedback from the three unilateral subjects participating in the study are generally neutral, with novel interfaces being evaluated as close in fit to conventional interfaces during sitting and standing. One bilateral patient rates the novel interface as better than the conventional interface on both legs. The three unilateral patients give the novel interfaces slightly worse ratings while walking, however often comfort was reduced due to unfamiliarity with the socket suspension system or socket material, neither of which are directly applicable to our design. Overall, study results show that the performance of the novel interface is comparable to that of the conventional interface with the potential of providing benefits in overall design time, repeatability, and cost.

Thesis Supervisor: Hugh Herr, Professor, Department of Media Arts and Sciences
Reader: Amos Winter, Associate Professor, Department of Mechanical Engineering

Acknowledgments

This thesis would not have been possible without the support of my mentors, friends, and family. I would first like to thank my advisor, Hugh Herr, for his support, guidance, and confidence in me throughout my time at MIT. A big thank you to my reader, Amos Winter, for his feedback and comments. Thank you to the labmates whom I worked with on this project: Xingbang Yang for showing me the ropes, guiding me through my first year, and laying the foundation for this project, Christina Meyer for all her work on the socket project and for helping me work through the code and errors that inevitably came up, and Francesca Riccio-Ackerman for all her support on the socket evaluation questionnaire and COUHES protocol minutiae. I would also like to thanks Eric Rasmussen for his help on the design code and Julia Howarth for her help in analyzing the evaluation data.

Thank you to Michael Fernandez for being a great roommate, helping me keep a good work-life balance, and making the graduate school experience more enjoyable. Also thanks to the 2022 MIT Mechanical Engineering master's cohort for being a wonderful group of people. These past two years, however difficult due to Covid, were made better through the people I have met along the way and I will be sad to see many of us go our separate ways.

To my mother and father: thank you for everything you have done for me, for raising me, believing in me, and always supporting me throughout my life. There is no way I would be here without you both, and I love you.

Contents

List of Figures

List of Tables

Chapter 1

Introduction

1.1 Motivation

Today there are more than 2 million people in the United States living with limb loss, with that number projected to grow to 3.6 million by 2050 [1, 2, 3]. People with disability are more likely to be at a socioeconomic disadvantage, show increased incidence of using emergency healthcare services, and express a worse outlook on overall health compared to those without disability [4]. Lower limb amputation is the most common type of amputation, with transtibial (below-knee) amputation making up a significant portion [5]. Reasons for transtibial amputation ranges from trauma to dysvascular disease, and with the increasing rates of diabetes worldwide, the population of transtibial amputees will only increase in the future [6, 7]. Amputation has long-lasting physical and mental effects, including chronic residual limb pain, phantom pain, and skin sores, diminishing quality of life, and exacerbating psychological problems. In a study of 92 participants living with lower-limb amputation, the fit of the socket was the primary concern with wearing a prosthesis, closely followed by the ability to walk on the prosthesis and avoidance of skin sores or rashes [8]. The secondary concerns are dependent on the primary.

The fit of a prosthesis is determined by the two major components of a socket: a soft liner and a rigid socket shell. The liner provides cushion between the skin and the socket while the socket shell supports the limb by distributing load in a comfortable

manner and providing structure, and stability. A proper socket fit will eliminate several of the aforementioned interrelated problems, and therefore it is imperative that each socket be uniquely tailored to its wearer.

1.1.1 Traditional Socket Design

The most common method of designing prosthetic sockets is highly artisanal, lacks scientific rationale, and involves extensive time from both patient and prosthetist [9]. A plaster cast is made of the patient's limb to get the surface geometry, and from this cast the prosthetist makes a positive mold of the residuum. The positive mold is used to make check sockets out of polycarbonate. The patient then tests the check socket and the prosthetist makes changes as needed. Once the patient is satisfied with the fit, another positive mold is made from the final check socket and this final positive is wrapped in carbon fiber to create the final socket [10]. Conventional prosthetic liners are usually generic items and are not patient-specific, meaning they are not shaped to match the user's residuum.

The quality of socket fit depends on the skill and experience of the prosthetist, which results in inequitable prosthetic care across varying income levels and geographic regions. Poor fit is so prevalent that 57% of prosthesis users report moderate to extreme pain, and up to 75% of lower-limb prosthesis users have experienced skin problems [11]. Rates of pain and irritation are higher among diabetic amputees than non-diabetic amputees, and this is especially concerning given diabetics' reduced ability to heal from injury [12].

Customizing socket fit is performed in several ways, with hand-modification being the most common. This also depends on the skill of the prosthetist, lacks any consistent scientific or medical method, and is not easily repeatable. Other attempts to address socket fit are through the development of variable-impedance sockets, 3D-scanning, and computer-aided modeling, but each of these has limiting shortcomings.

Due to the time requirements and cost of traditionally made sockets, patients are limited in what they can test and modify during the check socket period. Every change has to be done sequentially and extensive trial-and-error is involved. Active

prosthesis wearers need new sockets every 2-3 years, and this process has to repeated for every new socket. Individual socket preferences, such as regions of sensitivity not reflected in the skin geometry, must be manually reapplied to every new socket. The inefficiency of the process can result in periods where a patient's mobility is limited due to not having a well-fitting socket. This leads to some patients willing to live with limited mobility because they do not have time or resources to refit for a new socket.

1.2 Prior Art

There have been several attempts to improve transtibial prosthetic interface comfort and fit, most focusing on multi-material or variable impedance socket design. There also exist methods to make socket design less artisanal by using 3D scanning to eliminate the initial plaster casting step from traditional socket design.

1.2.1 Multi-material Sockets

Within the Biomechatronics group, multi-material variable impedance sockets have been created and tested from 3D models of transtibial residuums [9, 13]. These sockets use materials of different stiffness to alleviate high-pressure areas. Examples of these sockets are shown in Figure 1-1.

The required socket material impedance is determined by mapping the bone tissue depth of the residuum to the socket. These sockets demonstrated a reduction in socket-skin interface pressure during both walking and standing. Due to the limitations of multi-material additive manufacturing, these variable impedance sockets were much heavier than conventional carbon sockets. The socket materials were also prone to cracking and degradation as seen in Figure 1-2.

Other companies are also producing multi-material sockets to improve comfort. These include Hanger Clinic's ComfortFlex Adapt and Prosfit's Natural+Flex socket among others. Other solutions to improve fit include multi-piece sockets such as the RevoFit2 and Ottobock's Varos socket. These sockets consist of an inner section and

Figure 1-1 Two examples of multi-material sockets produced by the Biomechatronics group. They use different algorithms to determine areas of variable material compliance, and are both 3D-printed. The one on the right was the product of David Sengeh's Ph.D. thesis [13].

an outer shell that can be user-tightened to the proper fit.

1.2.2 3D Scanning

3D scanning the residuum topology has become a common alternative to traditional plaster casting. Various scanners can be used, such as hand scanners which rely on photogrammetry to reconstruct a 3D model. Prosfit's Pandofit socket pipeline utilizes 3D scanners to obtain the residuum skin geometry [14]. Many independent prosthetic clinics have also started using various available 3D scanning software to replace casting. While scanning is able to replicate the surface geometry, it cannot capture the bone geometry or soft tissue depth of the residuum, both of which are important to achieving optimal socket fit.

Figure 1-2 A crack in a multi-material socket that already lost the medial lobe due to material failure.

1.2.3 3D Printing

Check sockets do not need to be particularly robust or made out of expensive material, so 3D printing is increasingly used to fabricate these sockets. There are many agencies that take commissions to produce custom parts, such as Sculpteo, Xometry, Extremiti3D, etc. These companies usually have a variety of materials and a breadth of knowledge about printing to maximize the quality of the finished product. There are also many 3D printers on the market that can be used to print sockets. Large polyjet printers such as the Stratasys Connex series or HP Multi Jet Fusion can fabricate multi-material sockets in a single print. Biomechatronics has previously used an in-house Stratsys Connex 500 printer to print variable impedance sockets.

1.3 Previous Work

The codes used to digitally design prosthetic interfaces were first started in 2015 by members of the Biomechatronics group at the MIT Media Lab. The MRI pipeline consists of 10 codes (referred to as Demos) that process three-dimensional images sets to develop optimal socket and liner geometries [15]. The codes are all written and run in MATLAB. Figure 1-3 provides an overview of the full design pipeline cycle.

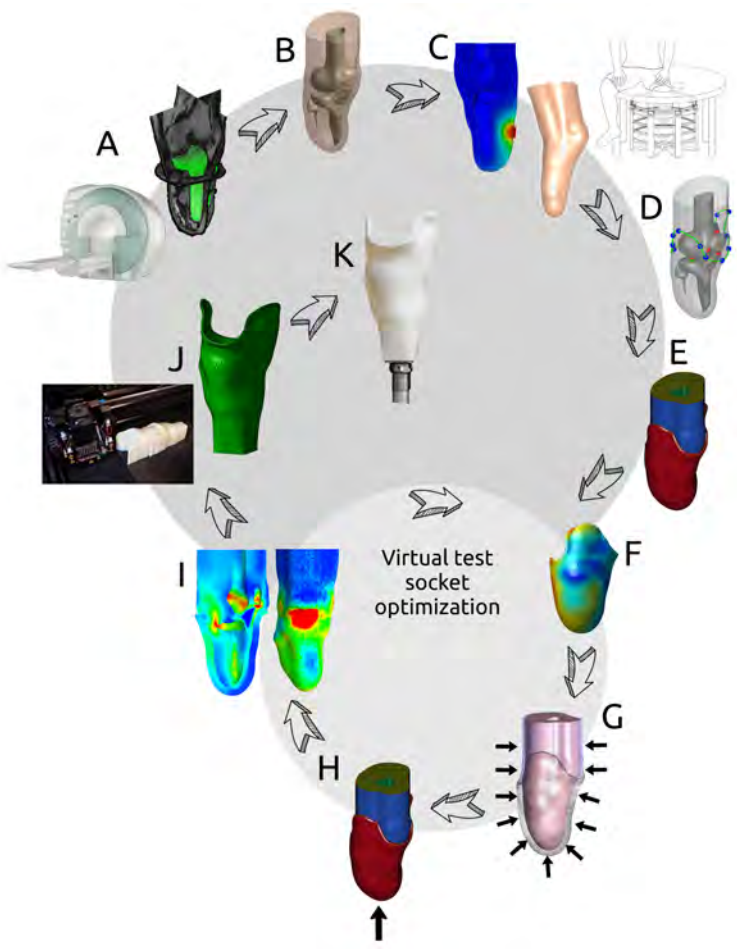

Figure 1-3 Updated version of Figure 3 from [15].

The 10 demos must be run sequentially, meaning that changes to an earlier code requires all subsequent codes to be rerun. The design steps are detailed below, divided into sections of related operations.

1.3.1 Limb Model Generation (Demos 1-6)

After the residuum is imaged, the image slices are segmented into corresponding anatomical structures using the GIBBON toolbox [16]. These structures are: skin, femur, tibia, fibula, patella, patellar tendon, and any locating MRI markers. A contour is generated for each image slice, and the contours are combined into a complete levelset once every slice has been completed. The levelsets are then meshed into three-dimensional surfaces and reoriented so that the positive (upward) z-axis matches the main axes of the femur and tibia and the positive (forward) x-axis is defined based on the femur and patella. The final step in model generation is to reconstruct the patellar tendon attachment points to the tibia and patella in order to ensure good contact with no gaps.

Because the MRI must be done with the patient lying prone, the MRI skin surface is deformed in a way that is not representative of the limb in a socket. To correct for this, a digital image correlation (DIC) system shown in 1-4 is used to capture accurate skin geometry while the limb is suspended [17, 18].

The limb is covered in white alcohol-based paint with a random black speckle pattern airbrushed on top. The DIC system uses cameras with overlapping fields of view to match speckle points between undeformed (straight) and deformed (bent) image sets. After all image sets are matched, a 3D point cloud is created. The point cloud is imported into Rhinoceros 5 3D modeling software, meshed, and any holes are patched and smoothed. The resulting surface is used in replacement of the MRI skin surface.

1.3.2 Socket and Liner Design Codes (Demos 7-10)

For each subject, individualized versions of Demos 7-10 are kept in order to retain any design changes made to sockets for that subject. Therefore successful changes will be applied to all future sockets for a subject, reducing need for iteration in successive socket fittings.

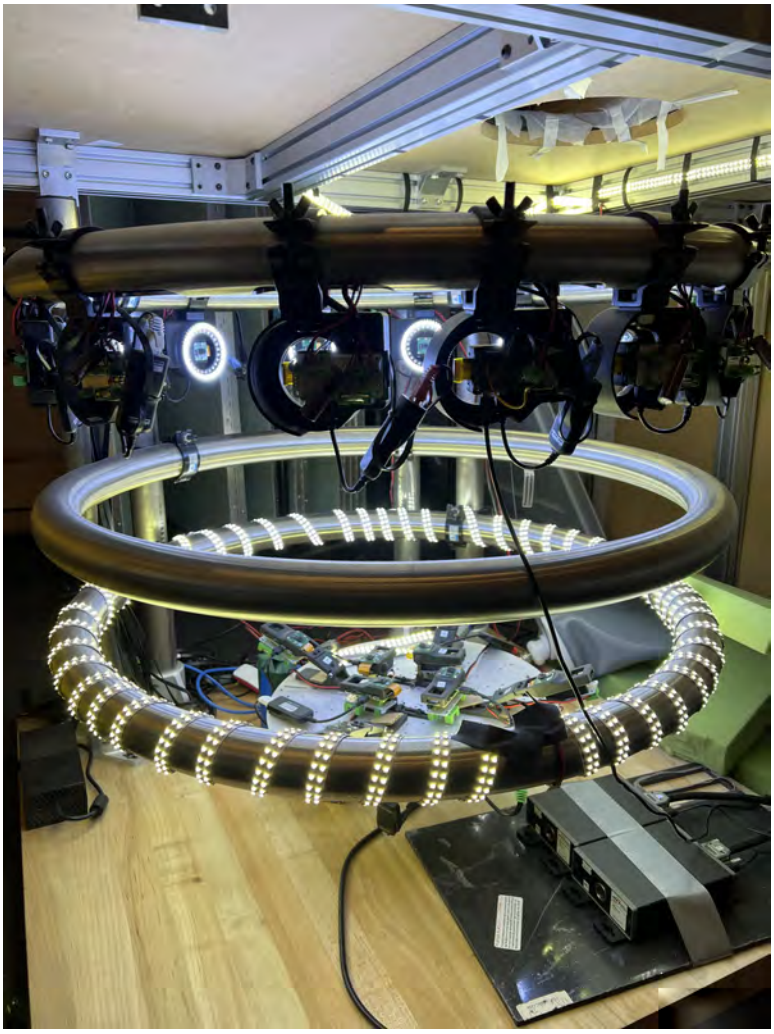

Figure 1-4 The digital image correlation system developed and used in Biomechatronics.

Socket Design Initialization (Demo 7)

Interface design begins by loading the MRI and DIC surfaces and using a reference femur to reorient the entire model. This ensures that the femoral head is vertically above the knee and femoral condyles so that load will be directed straight downward. There is the option to change loading directions if needed, but it is not used in this work. The model top is cut to a flat surface and meshed to create a closed 3D model. The liner surface is created by offsetting the skin surface by a defined distance. In this work, this distance is 7mm by default, but changes based on the actual thickness of the printed liner. The socket cutline is defined through 14 points based on anatomical

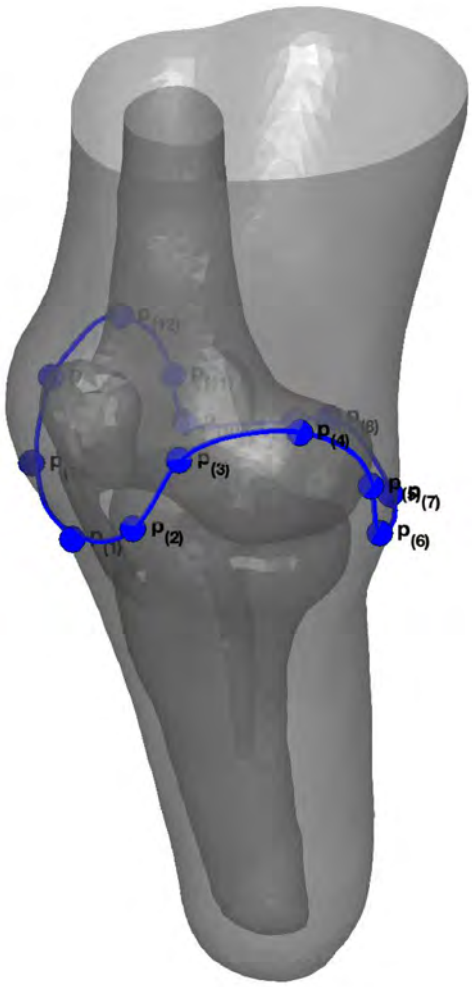

Figure 1-5 The 14 points that define the socket cutline. Point 1 is located at the center of the patellar tendon, and move to the medial then posterior then lateral sides (counter clockwise when viewed from top-down).

landmarks around the patellar tendon, femoral condyle, and tibial condyle regions, shown in Figure 1-5.

The socket surface is defined as the region below this cutline. The socket outer surface is then offset 8mm from the liner surface and a smooth mesh is applied to connect the socket inner and outer surfaces and create the socket model. The loadline is calculated from the head of the femur to the bottom of the socket, and should run through the center of the socket when seen from an anterior view in order to ensure proper alignment and stability. This code generates a mesh file with all the socket geometrical parameters. If anything about the liner thickness, socket cutline, or

loadline changes, Demo 7 has to be rerun to generate a new mesh.

Socket Pressure Region Definition (Demo 8)

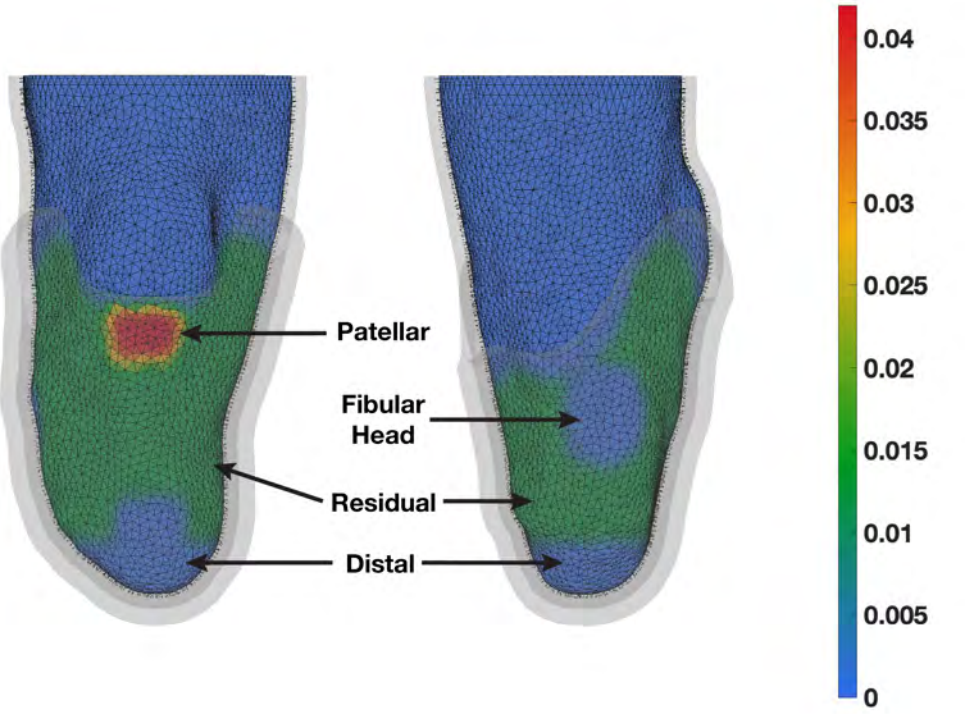

Figure 1-6 The pressure regions defined for FEA. The left image shows the anterior view and the right figure shows the lateral view. The scale bar shows the pressure in kPa.

To ensure the best socket fit, our algorithm uses finite element analysis (FEA) to apply differential pressures in the socket based on common sensitive regions and patient feedback. As the model has matured we have segmented the model into four main pressure regions. The first is the patellar tendon area, where the highest pressure is applied because this region can bear the most load [19]. The second and third regions are the distal end of the tibia and the fibular head protrusion. Both of these areas have 0 fitting pressure applied because they are the most sensitive regions of a transtibial residuum. We additionally add an extra window of 0 fitting pressure above the distal region at the anterior of the tibia because that is a common area of discomfort feedback from our patients. The final region is everything other than the

aforementioned regions, which we call the residual pressure region. This region bears the rest of load and holds the limb suspended in the socket. These regions can be seen in Figure 1-6.

Finite Element Analysis (Demo 8)

Finite element analysis is used to simulate loading the interface in order to get the optimal weight-bearing socket and liner geometries. We use the FEBio package along with GIBBON [20]. The FEA process consists of 5 steps, each simulating an equivalent real-world test:

1. Designing the liner: Liner fitting pressures are applied to the skin, causing deformation that defines the liner surface. This is done until the interface pressure between the liner nodes and skin nodes reaches specified values.

2. Donning the liner: After the liner and skin reach target pressure, the material properties of the liner are applied to the liner model. The geometry is retained but the pressure is reduced slowly, allowing the soft tissue to relax into the liner.

3. Designing the socket: Socket fitting pressures are applied to the liner model at the regions where the socket model exists, which deforms until target pressures are achieved.

4. Donning the socket: the socket model is given material properties and then pressures are ramped down, allowing the soft tissue and liner to relax into the socket.

5. Applying bodyweight: Bodyweight is applied to the limb-liner-socket model in the z-direction to simulate standing. This is done until a target reaction force is reached.

One iteration of FEA is run to produce the liner geometry. The liner is then converted to a Standard Tessellation Language (STL) file and printed. To get the most accurate socket geometry, the actual thickness of the liner is measured after

it is printed. This actual thickness value is then input into the liner and socket initialization code (Demo 7) and a new mesh is created. This is done because the silicone printing process used to fabricate the liners is still in its infancy and tolerances are not good enough to assume the liners are actually 7mm thick. Using the new mesh, we run FEA through 3 iterations of these steps to produce the final socket geometry. Three iterations was settled on after several test runs. After 1 iteration of FEA, new regions of high pressure may develop and regions where we want 0 pressure may not reach acceptable levels. These are rare occurrences, but we have found 3 iterations is the most reliable in producing consistent pressures.

Socket Modification (Demo 9)

After running FEA, the final socket and liner geometries are smoothed and converted to STLs for 3D printing. In this step, manual changes can be made to the socket geometry. These include manipulating nodes, fixing curvature, smoothing, and defining the print thickness. Demo 9 also lengthens the liner by extruding the top of the liner beyond the top of the model. Modifications to this code are detailed in the experimental design section. The result of Demo 9 are the final socket and liner geometries.

Socket Compilation and Positive Plugs (Demo 10)

Part A of Demo 10 has the ability to organize multiple socket STLs into a single file for printing. It also renames STL files and compiles multiple files into one output folder for convenience. For this work, the printer required each socket to be in its own file so Demo 10a was only used to compile and consistently name sockets sent out for printing.

Part B of Demo 10 designs a positive mold for a successful socket. This code is only run once sockets have been fit, walked in, and approved by patient and prosthetist. The geometry of the successful socket is imported and the socket inner surface is used as the outer surface of the mold. This positive mold can then be used to make a permanent carbon socket. Construction of permanent daily-use sockets is not the

aim of this project, so Demo 10b is not used.

1.4 Research Objectives

The prosthetic interface fit is often the limiting factor in prosthetic use and user comfort, and therefore improving fit will have far-reaching benefits for the community of people with amputation. Custom, user-specific liners will be an improvement over generic liners of today. Furthermore, socket fit is heavily dependent on the prosthetist who designs it, meaning those without means are inherently disadvantaged when it comes to prosthetic care. The aim of this work and this thesis is to make the prosthetic interface design process more scientific and repeatable and simultaneously reduce the required time from the patient and prosthetist. Specifically, the ability to retain information about socket preferences uniquely to each patient will markedly reduce the time necessary to produce replacement or alternate sockets. These benefits will help democratize the prosthetic interface design process and increase access to good prosthetic care. We believe that through our process we can create novel prosthetic interfaces that are as comfortable or more comfortable than subjects' conventional interfaces during a sitting, standing, and walking evaluation. Four metrics are used to assess comfort: kinematic gait symmetry, skin temperature, relative socket interface pressure, and qualitative subject feedback through a questionnaire. Weight is given more heavily to the patient's qualitative feedback, as this is the most indicative of what the patient actually experiences. This thesis details the novel digital prosthetic interface design process and fabrication, and compares the comfort performance of our novel sockets against that of conventional sockets for several subjects.

Chapter 2

Socket Design and Evaluation

2.1 Modifications in Demos 7-9

2.1.1 Demo 7

The main changes made in Demo 7 are to the liner thickness and the socket cutline. Actual liner thickness of the printed liner is measured using calipers. The liner is sandwiched between between metal plates and measurements are taken at 5 different locations along the edge of the liner, as shown in Figure 2-1.

These values are averaged to get an estimated value for the liner thickness. The liner is always worn with a thin 0.5mm nylon sleeve to reduce friction between the liner and socket, so 0.5mm is added to the averaged thickness. This actual thickness value is then input into the liner and socket initialization code (Demo 7) and a new mesh is created. The socket cutline points can be manipulated in order to address various discomforts in the socket. A common change is raising the medial/lateral lobes of the cutline in the z-direction in the case where the subject feels unstable, shown in Figure 2-2.

The top of the lobes are usually raised anywhere from 1-3cm, with adjacent nodes being raised less to transition smoothly with the rest of the cutline This is commonly done for subjects with shorter residuums, as the shallow depth of the socket provides less inherent stability. The posterior section of the cutline is also frequently lowered

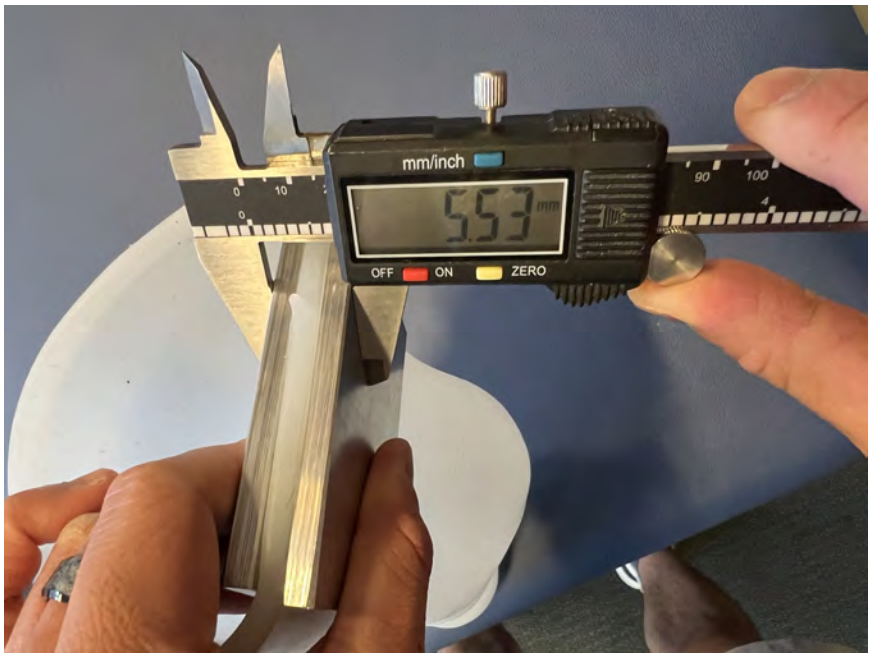

Figure 2-1 Liner Thickness Measurement Technique

3-5mm as it can dig into the skin when the leg is bent. The anterior node of the cutline is lowered 5mm for all subjects in order to not impinge the patella during knee flexion, as this can lead to injury during extended use.

2.1.2 Demo 8

Design changes in Demo 8 focus on manipulation of pressure regions for FEA. The first major change to all subjects is the aforementioned inclusion of a window of 0 fitting pressure above the distal region at the anterior of the tibia. This window is aligned with the anterior tibia by defining the centerline direction of the tibia, shown in 2-3.

The window extends a specified height, in mm, above the minimum point of the tibia and $\pm 1/2$ the specified width on either side of the centerline. The region of 0 fitting pressure around the fibular head protrusion can also be altered as this is a common area of sensitivity among transtibial subjects. The region of 0 fitting pressure around the fibular head can also be changed to accommodate subjects who are particularly sensitive in that area. The fibular head region is defined as an ellipse

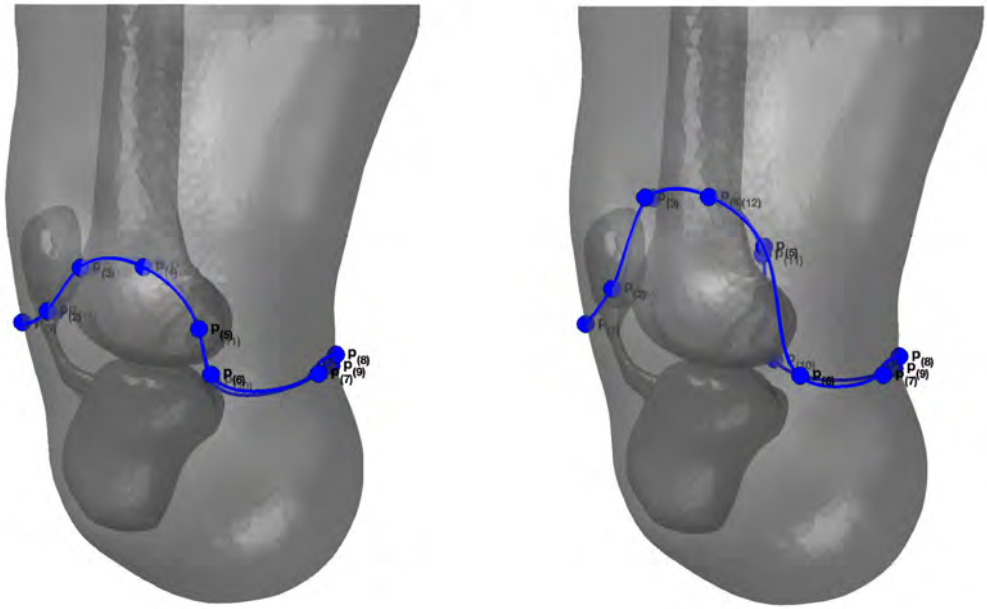

(a) (b)

Figure 2-2 Raising the medial-lateral lobes of the socket cutline. Figure 2-2a shows the default lobe height and Figure 2-2b demonstrates the raised lobes to increase stability for short residuums.

with one focus centered at the fibular head and the other a specified distance below it 2-4.

The ellipse can be expanded and translated as needed to minimize pain in that region. The four major pressure regions (patellar bar, distal, fibular head, and residual) are the default and sockets for new subjects only include these. We retain the ability to add additional regions of reduced pressure based on feedback from the subject from socket fitting and testing.

Once the pressure regions are defined, the pressure in each region can be adjusted independently. This is the primary way sockets are differentiated to search for a best fit. The base pressure is defined as 15kPa, and pressures are determined as multiples of this base pressure. For example, a pressure of 3x would mean the model aims to apply 45kPa in that area during FEA. Pressures will be described as a set

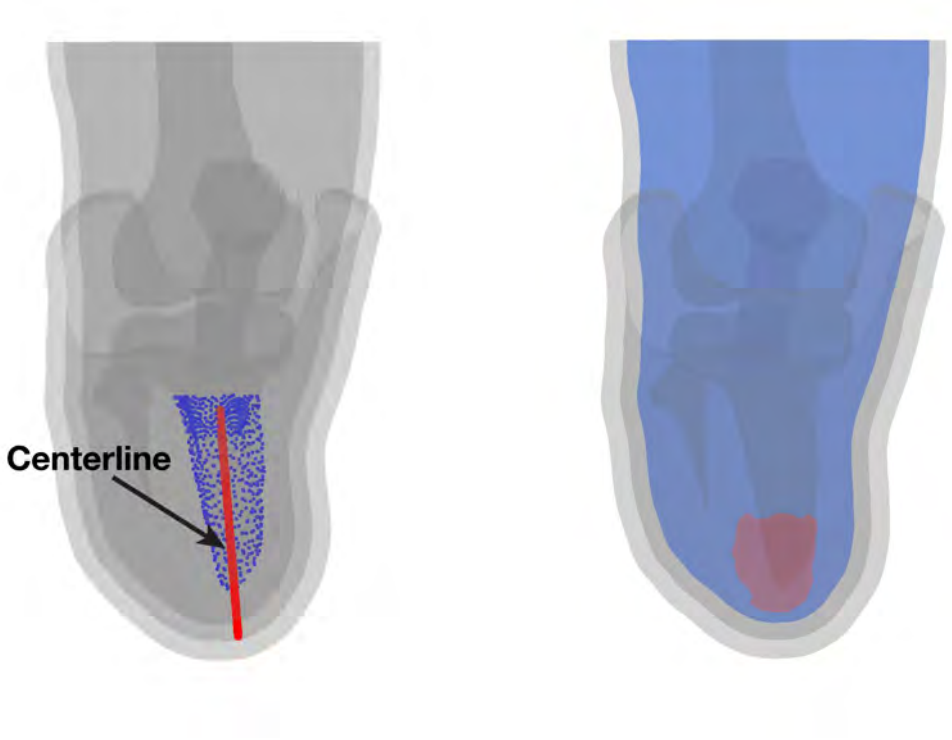

(a) (b)

Figure 2-3 Definition of the distal added pressure window. Figure 2-3a shows the centerline definition calculated based on the principal direction of the tibia using the nodes of the tibia. Figure 2-3b shows in red the window added to the distal region.

of three pressure multiples of the base pressure: distal/patellar bar/residual. Distal and fibular head pressures are the same. A socket described as 0x/3.2x/1.2x would mean that FEA aims for pressures of 0 at the distal and fibular head, 3.2 times the base at the patellar bar, and 1.2 times the base everywhere else on the socket. A socket set for a new subject consists of 3 sockets at three different pressure levels. To try to best ensure at least one reasonable fit, from experience these sockets are usually: 0x/3.0x/1.0x, 0x/3.2x/1.2x, and 0x/3.4x/1.4x. Pressures are then increased if the socket is too loose or decreased if the socket is too tight. The difference of 2x between patellar bar and residual pressures is not fixed and can be changed based on the subject. However, it is normally kept at 2x unless the socket fitting pressures get unusually high or unusually low.

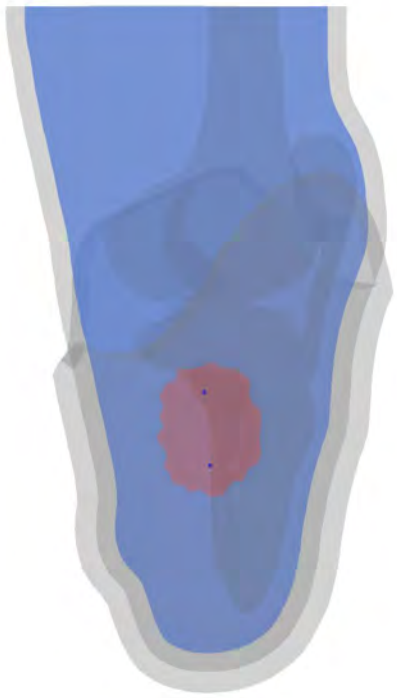

Figure 2-4 The fibula head pressure region definition

2.1.3 Demo 9

Demo 9 allows for the most flexibility in design changes to the socket. The most common complaint received is excessive pressure at the distal end of the tibia, even after 0 fitting pressure is applied during FEA. Therefore it is standard practice to pull out nodes at the distal end 3mm, with a gradient applied to smoothly integrate the modification with the socket. Other modifications that are used are tibial medial flare and fibular head enlargement. We retain this ability to pull out nodes arbitrary amounts anywhere on the socket, tailoring the socket to the subject. These changes are stored in the algorithm so that all sockets for a particular subject retain the modifications. We also smooth the socket surfaces in order to avoid sharp edges or corners. A Laplacian smoothing method is used for the upper section of the socket. We found at regions of high curvature, specifically the distal end, this method over-smoothed and started reducing the depth of the socket and potentially creating pain

at the distal end of the tibia. To correct this, we implemented a Taubin smoothing method at the distal end of the socket only. The difference between the two methods is that Taubin smoothing alternates the Laplacian smoothing operation with an expanding operation to counteract volume shrinkage from smoothing [21]. To separate the socket into distal and proximal sections, the distal pressure region is imported from the FEA results. The highest z-coordinate of the distal region, usually the top of the anterior tibia window, is used as the dividing height. A curve at that z-level is ray traced around the socket, the mesh is rearranged above and below this line, and the boundary region is smoothed. Then the two regions are then independent of each other as seen in Figure 2-5 and can be smoothed separately.

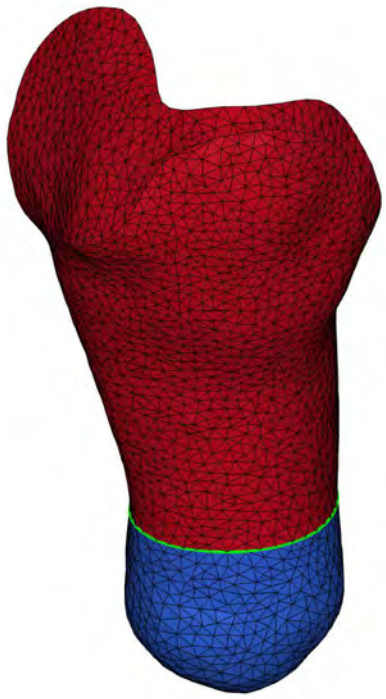

Figure 2-5 The separate distal and proximal socket regions. Red is proximal, blue is distal and the green line is the defined dividing line.

Demo 9 also extends the top of the liner beyond the top of the 3D model. Transtibial prosthetic liners ride up to mid-thigh level, and because the information contained

in the 3D model ends just above the knee it is necessary to extend the liner. This is done by defining a curve 100mm above the top of the liner top curve. This upper curve is a circle of circumference measured at the subject's mid-thigh. The liner is then extended using a linear flare between the two curves.

2.1.4 Fabrication

After final modification and compilation, the liner STL is sent to Rapid Liquid Print (RLP) and the socket STLs are sent to Extremiti 3D for printing (also known as additive manufacturing, or AM). Extremiti 3D uses AM to fabricate check sockets out of PCTG. PCTG is an impact-resistant thermoplastic polyester that exhibits lower shrinkage and higher temperature resistance compared to its more common sibling PETG, and these benefits make it ideal for printing check sockets with high dimensional fidelity [22]. Additive manufacturing allows the printing of several variations of a socket at once, and is less expensive than traditional check socket fabrication. It also has much shorter lead times compared to traditional molding for highly custom parts such as sockets. RLP prints liners out of platinum-cure silicone at a nominal thickness of 7mm. 3D printing of soft materials of very low durometers is still in its infancy, so corrections need to be made based on the actual print thickness as described above.

Check sockets are printed at a thickness of 8 mm to prevent cracking during fitting. However, the sockets are not airtight immediately after printing, which prevents a vacuum from forming and causing pistoning in the socket. Pistoning is the phenomenon when the limb moves vertically within the socket, causing discomfort, instability, and insecurity with socket fit [23]. To correct this, the distal end of the socket is taped with electrical tape during initial fitting, and then coated in epoxy when a pyramid is attached for walking.

2.2 Socket Evaluation

Four subjects consisting of 5 residual limbs were evaluated in this study. Birth year, sex, activity level, and cause of amputation are listed in Table 2.1 below:

Subject	Birth Year	Sex	Activity	Side	Cause
1	1964	M	K4	Bilateral	Trauma
2	1971	M	K4	Right	Trauma
3	1975	M	K4	Left	Trauma
4	1990	F	K4	Left	Trauma

Table 2.1 Study subject information

All were approved by the Committee on the Use of Humans as Experimental Subjects at the Massachusetts Institute of Technology. In this paper I will use the words patient and subject interchangeably.

2.2.1 Socket Fitting

Check sockets are printed with no foot attachment point, as shown in Figure 2-6a.

This is done because optimal alignment is not yet known for each subject. The subjects first test the standing fit of the sockets in lab using a height-adjustable platform to achieve approximate level standing. The standard procedure is to produce three sockets that are identical apart from increasing fitting pressure. The subject will test each socket to ensure that at least one provides a good fit. If the subject fits one of the sockets, we take any feedback on pain points or high-pressure regions to design two to three more sockets based on the best-fitting socket. The subject will then test these three sockets with CPO Bob Emerson at A Step Ahead Prosthetics to get a professional evaluation. Minor manual modifications (grinding, blowing) are acceptable, with the regions and operations recorded to make changes to the computational model. 1-ply socks are also acceptable to counteract natural limb shrinkage over the course of the day. The prosthetist will then align the best-fitting socket and attach a pyramid connection point to the distal end, as seen in 2-6b. The subject will proceed to attach their foot-ankle component to the novel socket and test

(a) (b)

Figure 2-6 Novel sockets before and after socket fitting. The socket in Figure 2-6a is shown as received directly from Extremiti3D with no pyramid attachment. Figure 2-6b is an aligned socket, fitted with a pyramid and attached to a pylon for walking. No foot/ankle system is attached.

walking for 10-15 minutes. Suspension is achieved using a high density, 3 mm thick suspension sleeve from Alps South LLC. If there are uncorrectable pain points while walking, we will take all changes and feedback into account and redesign three more sockets before returning to the prosthetist for another fitting. If the subject deems the socket comfortable both standing and walking, we proceed to evaluation.

2.2.2 Kinematic Evaluation

One method to evaluate the prosthetic interface fit is gait symmetry. To measure this, kinematic walking data is collected using motion capture. At the Biomechatronics lab this is done using a Vicon system. The subject is asked to walk with their conventional system on a treadmill for 5 minutes at 1.3 m/s. During the 5 minutes, three 30-second data collections are made. Immediately after the 5 minutes walking, the socket and liner are doffed for thermal imaging. The conventional socket is then removed from

the foot/ankle system and the novel socket is attached. This 5-minute walking trial is then completed with the novel socket and liner on the same foot/ankle system. A note for Subject 2 is that his daily use prosthetic is a monocoque socket+blade foot system, so it is incompatible with the testing method of switching sockets on the same foot/ankle. Therefore Subject 2 has to use an alternate prosthesis with a different foot/ankle that he mainly uses to ski. The socket geometry for this alternate is the same, but the subject is not as used to walking with the foot/ankle system used in the evaluation.

Gait symmetry is evaluated by comparing gait metrics between affected and unaffected sides. The metrics used in this study are:

- Step Time: Defined as heelstrike of one foot to heelstrike of the contralateral foot.
- Swing: Defined as toe-off to heelstrike of the same foot.
- Impact Peak Ground Reaction Force (GRF): The peak magnitude of force in the vertical (Z) direction applied after heelstrike.

For each subject, gait metric data is split into right and left sides. Based on prior gait studies [24], a measure of asymmetry is the percent difference between metrics from sequential steps on each side. For this study we are concerned with direction of asymmetry, so the modified metric used here is given by Equation 2.1:

$$\%Asymmetry = \frac{Affected - Unaffected}{mean(Affected + Unaffected)} \tag{2.1}$$

The asymmetry percentage is calculated for sequential steps for each metric. For example, if the data collection begins with a right-led step, the corresponding asymmetry percentage will be calculated using the metric for that step and the metric for the left-led step immediately following. This is done for all walking data for each subject.

Ramakrishnan et al. also give a combined gait asymmetry metric (CGAM) based on various gait parameters [25]. The CGAM used is the Mahalanobis distance, given

by Equation 2.2, which determines the distance of points in a dataset to those in another reference dataset.

$$D = \sqrt{(Data - \mu) * \Sigma^{-1} * (Data - \mu)'} \tag{2.2}$$

In Equation 2.2, μ is the average of the reference and Σ is the covariance matrix of the dataset. The apostrophe after $(Data - \mu)'$ means transpose. For this study, the Mahalanobis distances are calculated based on the asymmetry percentages of the 3 different metrics described above, giving 3 degrees of freedom. The conventional data is used as the reference so the Mahalanobis distance is calculated for every point in the novel data.

2.2.3 Thermal Evaluation

There is a correlation between skin surface pressure and temperature, so thermal imaging of the residuum is used to compare interface fit [26]. A Flir E4 thermal camera is used. When the subject first arrives in lab, they doff the conventional system and wait 10 minutes to allow the residuum to normalize. Four reference images (anterior, posterior, medial, lateral) are taken of the limb from 0.5 meters away. After the subject completes the first 5-min walking trial, the interface is doffed and images are immediately taken to best capture the skin temperatures caused by the conventional system. Another 10 minutes is given to allow the limb to cool, and a second set of reference images is taken. The process is repeated after the second walking trial, for a total of 16 images.

Images are grouped by position so that each position has a reference, conventional, and novel image. Images are imported into MATLAB and cropped to the area of concern in order to reduce unwanted information. The cropped images are converted into color heat maps based on the temperature scale from the camera. For each image a total average temperature is calculated, as well as temperatures at 6 chosen locations on the limb. These spots are chosen in the pattern shown in 2-7 below so there is 1 distal, 2 at mid-tibia level, 2 at fibular head level, and 1 near the patellar

tendon.

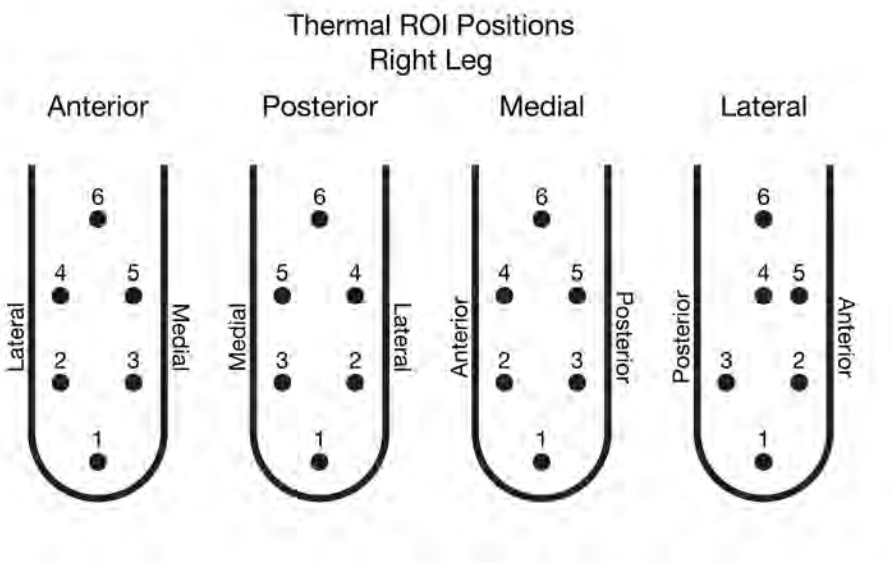

Figure 2-7 The layout of the 6 regions of interest for each image direction of the right leg for thermal data processing. The positions would be mirrored for a left-affected subject.

Total average residuum temperature due conventional and novel systems is compared by calculating the percent change in temperature from reference and then conducting a Mann-Whitney U-test to compare the two datasets [27]. Percent change is given by Equation 2.3 and is calculated for each subject by interface type and view direction (anterior, posterior, medial, lateral), giving two datasets of n=5 per view direction, one for conventional and one for novel. In Equation 2.3, $Final$ is either the conventional or novel temperature value and $Reference$ is the reference temperature. The Mann-Whitney U-test is non-parametric (no assumption of normality) and is chosen due to the small size of the datasets. The null hypothesis is that the datasets are not statistically different, and a significance level of 0.05 is used.

$$\%Change = \frac{Final - Reference}{Reference} * 100 \tag{2.3}$$

A comparison test is conducted for each view direction and also for a combined dataset of all view directions with n=20, giving 5 total decisions on whether to reject the null hypothesis. The same statistical analysis is performed on the distal and

fibular head regions of interest, as those are the locations that we are most concerned with reducing pressure.

To get a better sense of the direct comparison between conventional and novel temperatures, the percent difference is calculated using Equation 2.4

$$\%Difference = \frac{Conventional - Novel}{mean(Conventional + Novel)} * 100 \tag{2.4}$$

2.2.4 Pressure Evaluation

The pressure exerted by the prosthetic interface on the skin is a measure of fit, with lower pressure indicating a better geometrical fit. Excluding the patellar bar, consistency in pressure in the rest of the socket also indicates even distribution of load. We leave the patellar bar out because it can bear more load than the rest of the residuum. Relative pressure between the conventional and novel systems is measured using Tekscan Flexiforce A101 force-sensitive resistors, calibrated using an Arduino Mega and potentiometers. The sensors are taped to six locations on the residuum: patellar tendon, fibular head, anterior mid tibia, anterior distal tibia, posterior proximal wall, and posterior distal wall as shown in Figure 2-8 below.

Starting with the conventional system, the liner is carefully rolled over the sensors and then the socket is donned. The subject then stands with weight on the affected limb and the sensors are checked and calibrated to ensure that all are functioning and none are maxed out. Data collection consists of a 90-second standing trial made up of 30 seconds on the affected leg, 30 seconds on both legs, and 30 seconds back on the affected leg. This is done to ensure consistent measurement of the affected leg after unloading and reloading weight. The conventional system is then doffed and the novel system is donned. Without recalibrating any of the sensors to ensure proper relative comparison, the 90-second trial is completed with the novel system. If any sensor disconnects or is pinned high (maxed) during swap or second trial, the sensor circuit must be repaired and/or recalibrated and the entire process is repeated.

Pressure data is cleaned by averaging out any intermittent 0 values, taking a moving average, and plotting the conventional and novel signals on top of one another

(a) (b)

Figure 2-8 Pressure sensors attached to the 6 locations on the residuum of Subject 4. 2-8a is the anterior view showing three of the sensors, 2-8b is the posterior view showing the other three.

for each location. Data is narrowed down using a specified time window to isolate each approximate 30-second time period. These windows can vary from 20 to 30s based on how accurately the subject switched stance from single leg to double leg and back. The signals within each window are then normalized by the overall peak value of both signals. Within these windows, the section of least total variance between both the conventional and novel is found as this is the time frame where the subject is standing stable. Figure 2-9 shows an example of this section of least variance within a time window.

From experimentation, a 6-second window of least variance is determined to be best. The average values are found for both novel and conventional sockets in this 6-second window, expressed as a percentage of the overall maximum value. Therefore a lower percentage of the overall maximum indicates lower pressure.

To measure consistency of pressure, the variance is taken for the 5 locations excluding the patellar bar (4 locations for Subject 4 due to an error with the fibular

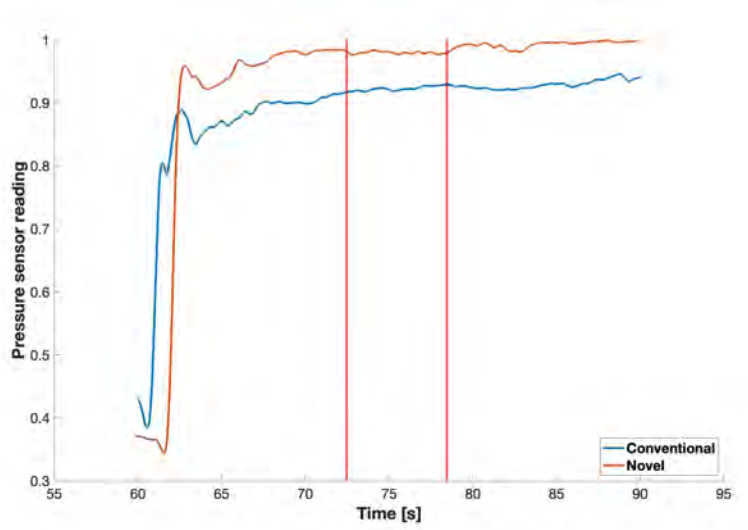

Figure 2-9 The 6-second window of least variance within a pressure trial, marked by the two red lines. The pressures during this time are used to determine the average values for comparison.

head sensor). Variance is given by Equation 2.5 where S^2 is the variance, x_i is one pressure value, μ is the average value, and n is the number of values.

$$S^2 = \frac{\Sigma(x_i - \mu)^2}{n - 1} \tag{2.5}$$

This gives two variances for each subject, one for the conventional socket and one for the novel. A Mann-Whitney U-test is again used to statistically compare the variance datasets, with null hypothesis that the datasets are not statistically different and a significance level of 0.05.

2.2.5 Questionnaire

Questionnaires are commonly used in prosthetics research to get direct subject feedback about prosthetic fit and function [28]. A socket evaluation questionnaire (SEQ) is used to get a qualitative comparison between the subject's conventional system and our novel system. The SEQ is completed immediately after walking at the prosthetist office, barring extenuating circumstances. The SEQ first has the subject describe their conventional system use case and history. This includes lifestyle limitations due to

the socket or liner, pain points, skin irritations, other complaints, and overall satisfaction with their interface. The subject is then asked to rate the novel socket in comparison to their conventional socket in sitting, standing, and walking. Ratings are requested for 10 different regions of the socket. The aim is for the subject to, as best they can, isolate the fit and feeling of the socket and liner from any other aspect of the prosthesis, such as alignment, suspension, or foot/ankle feel.

Chapter 3

Results

Final socket pressures, as defined in Section 2.1.2, for the sockets used in evaluation are listed in Table 3.1 below.

Subject	Distal	Patellar	Residual
1R	0x	3.5x	1.5x
1L	0x	3.2x	1.2x
2	0x	4.2x	2.6x
3	0x	3.2x	1.2x
4	0x	3.8x	1.8x

Table 3.1 Final socket pressures.

3.1 Kinematic Evaluation

Gait symmetry analysis is performed on all 4 subjects. We recognize that the bilateral subject will have a more even symmetry due to both sides being affected, but their data is included as symmetry is being compared between novel and conventional sockets which still applies to bilateral subjects. The metric for symmetry is given by Equation 2.1. In the case of bilateral subjects, affected is substituted by right and unaffected by left. Numbers closer to 0, on either side, indicate a higher degree of symmetry.

3.1.1 Combined Gait Asymmetry Metric

The Mahalanobis Distance with 3 degrees of freedom is used as a combined gait asymmetry metric to evaluate the difference between conventional and novel sockets. The distance is defined using Equation 2.2 with the conventional dataset as the reference and distances calculated for novel dataset. The 3 degrees of freedom are the asymmetries for step time, swing time, and peak ground reaction force. Table 3.2 shows the average Mahalanobis distance as well as the maximum distance for each subject. Maximum distance is the novel socket step that is furthest away from the conventional dataset.

Subject	Average Mahalanobis	Max Mahalanobis
1	1.69	3.19
2	2.28	4.40
3	1.63	3.26
4	2.64	4.44

Table 3.2 Combined Gait Asymmetry Metric Results

The Mahalanobis distance is based on a χ^2 distribution, so critical values of χ^2 can be used to evaluate the above values. For 3 degrees of freedom, the critical χ^2 value is 7.815 for a significance level of $\alpha = 0.05$, which means any value greater than 7.815 is a multivariate outlier [29]. None of the subjects have an average distance greater than the critical value, and in addition none of the subjects have a maximum distance that is greater than the critical value.

3.1.2 Step Time

Average step time asymmetries for conventional and novel sockets are given in Table 3.3 as well as the difference in asymmetry from conventional to novel. A negative value in difference means on the novel socket the subject preferred their unaffected side more than their affected side compared to on the conventional socket and vice versa. We expect unilateral subjects to favor their unaffected side when walking,

Subject	Conventional Step Asym (%)	Novel Step Asym (%)	Difference (%)
1	0.63	-0.27	-0.90
2	-1.22	-3.47	-2.25
3	-3.47	-3.11	0.36
4	-2.44	-5.16	-2.72

Table 3.3 Step time asymmetry results

which is indicated by a negative asymmetry percentage. This is corroborated by the data, which shows that the unilateral subjects 2, 3, and 4 all favor their unaffected side. Subject 1 is much more symmetric than the other subjects, which is expected from a bilateral subject for step times. Subjects 1 and 3 have slightly more symmetric steps while wearing the novel socket while subjects 2 and 4 have more asymmetric steps.

3.1.3 Swing Time

Subject	Conventional Swing Asym (%)	Novel Swing Asym (%)	Difference (%)
1	-0.95	0.34	1.29
2	1.13	1.64	0.51
3	4.62	5.14	0.52
4	0.90	4.39	3.49

Table 3.4 Swing time asymmetry results

Table 3.4 shows average swing time asymmetries and the difference in averages for conventional and novel sockets. Swing time asymmetry is positive if the affected swing is longer than the unaffected. Based on how the asymmetry metric is defined, swing time asymmetry is expected to be positive for unilateral amputees. This is because swing time is equivalent to opposite foot single support time. It is expected that a unilateral amputee will spend longer on their unaffected side compared to their affected side, which means that they will have a longer swing time on their affected side compared to their unaffected side. Again, a bilateral amputee is expected to be

more symmetric than a unilateral amputee, which is confirmed here. All subjects have positive differences, meaning their affected swing time increases relative to their unaffected swing time (or right time increases relative to left for Subject 1) when switching from conventional to novel sockets. For Subject 1 this improves swing time symmetry. Subjects 2 and 3 show minor reductions in swing time symmetry on the novel socket, while Subject 4 shows a major reduction in symmetry.

3.1.4 Ground Reaction Force

Subject	Conventional GRF Asym (%)	Novel GRF Asym (%)	Difference (%)
1	-5.08	-3.12	1.96
2	0.13	1.16	1.03
3	2.68	2.89	0.21
4	-2.57	-2.04	0.53

Table 3.5 Peak ground reaction force asymmetry results

Impact Peak Ground Reaction Force asymmetry data is given in Table 3.5. Raw data is imported from force plates and smoothed using a Gaussian method. Figure 3-1 shows a raw signal for a walking trial and the extracted peaks for one side of the trial.

GRFs differ from step and swing time in that there are no general presumptions for unilateral or bilateral subjects. Impact GRFs are mainly determined by any pain points the subject feels on the affected side. If discomfort is triggered by harsh impact, a subject will likely reduce impact GRF to lessen this pain. GRF can also be affected by limited ankle flexion of the prosthetic foot, and all subjects in this study use passive foot-ankle systems. Negative GRF asymmetries indicate less impact on the affected (right in the bilateral case) side compared to the unaffected side. Subject 1 and 4 show improvements in symmetry when using the novel socket, while subjects 2 and 3 are more asymmetric on the novel socket. Of the unilateral subjects, two have increased impact force on their affected sides while one has decreased impact.

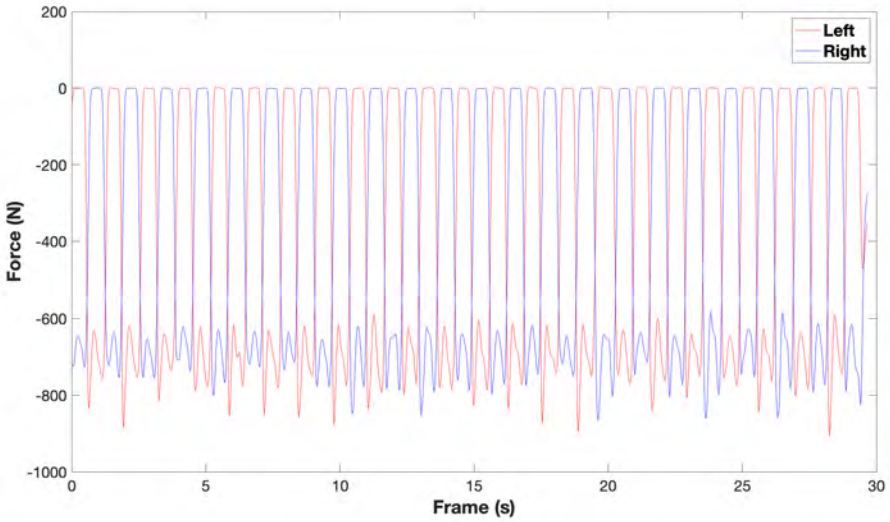

(a)

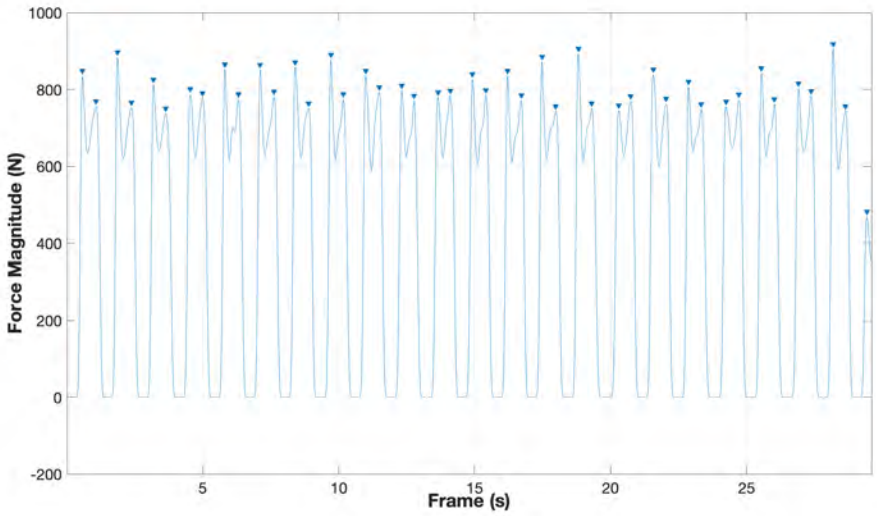

(b)

Figure 3-1 Figure 3-1a is a smoothed GRF dataset for one walking trial. Y-axis is force in N and X-axis is time. Values are negative because impact force is in the negative Z-direction. Figure 3-1b shows the found peaks for each gait cycle. Normal gait cycles will have two peaks, the first for initial impact and the second for powered push-off. The peaks included in this study are the first peaks of each cycle, which are the initial impact peak force.

3.2 Thermal Evaluation

For each position (anterior, posterior, medial, lateral), overall residual limb average temperature is calculated for reference, conventional, and novel images. Reference images are taken before a trial after the limb has been allowed to cool without a socket/liner system. Conventional and novel images are taken immediately after a walking trial on the respective system.

Figure 3-2 shows an example of the thermal image for reference, conventional, and novel trials.

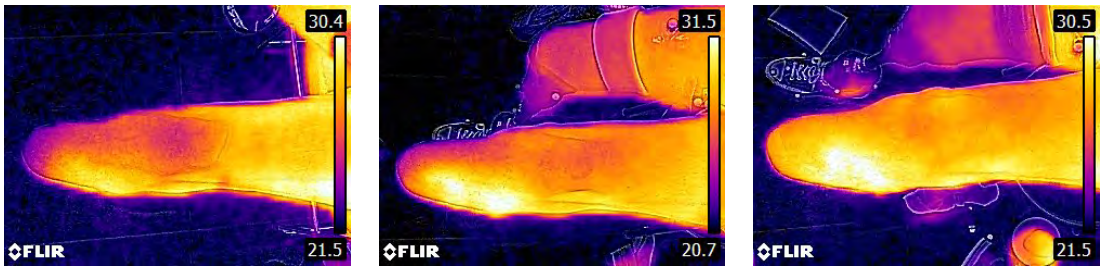

(a) Reference (b) Conventional (c) Novel

Figure 3-2 Example thermal images straight out of the thermal camera. Subject 1 right leg, anterior view.

These images are cropped and processed to extract temperatures from the residual limb only. Each image is scaled using its own color bar to give accurate temperature readings. Figure 3-3 gives the average temperatures for all residual limbs in the study for reference, conventional, and novel for each location.

Overall, there is generally a slight increase in residuum temperature from reference to conventional, and from conventional to novel. It is interesting to note the for Subject 1's right leg (1R), the reference temperature is consistently higher than the conventional and novel temperatures across all locations.

To compare the conventional and novel datasets statistically, the method described in 2.2.3 is used. Percent change from reference for conventional is given in Table A.1 and for novel in Table A.2. Decisions and p-values for comparing conventional and novel percent changes are given in Table 3.6.

Thermal data was also collected for 6 individual regions of interest (ROIs) on the

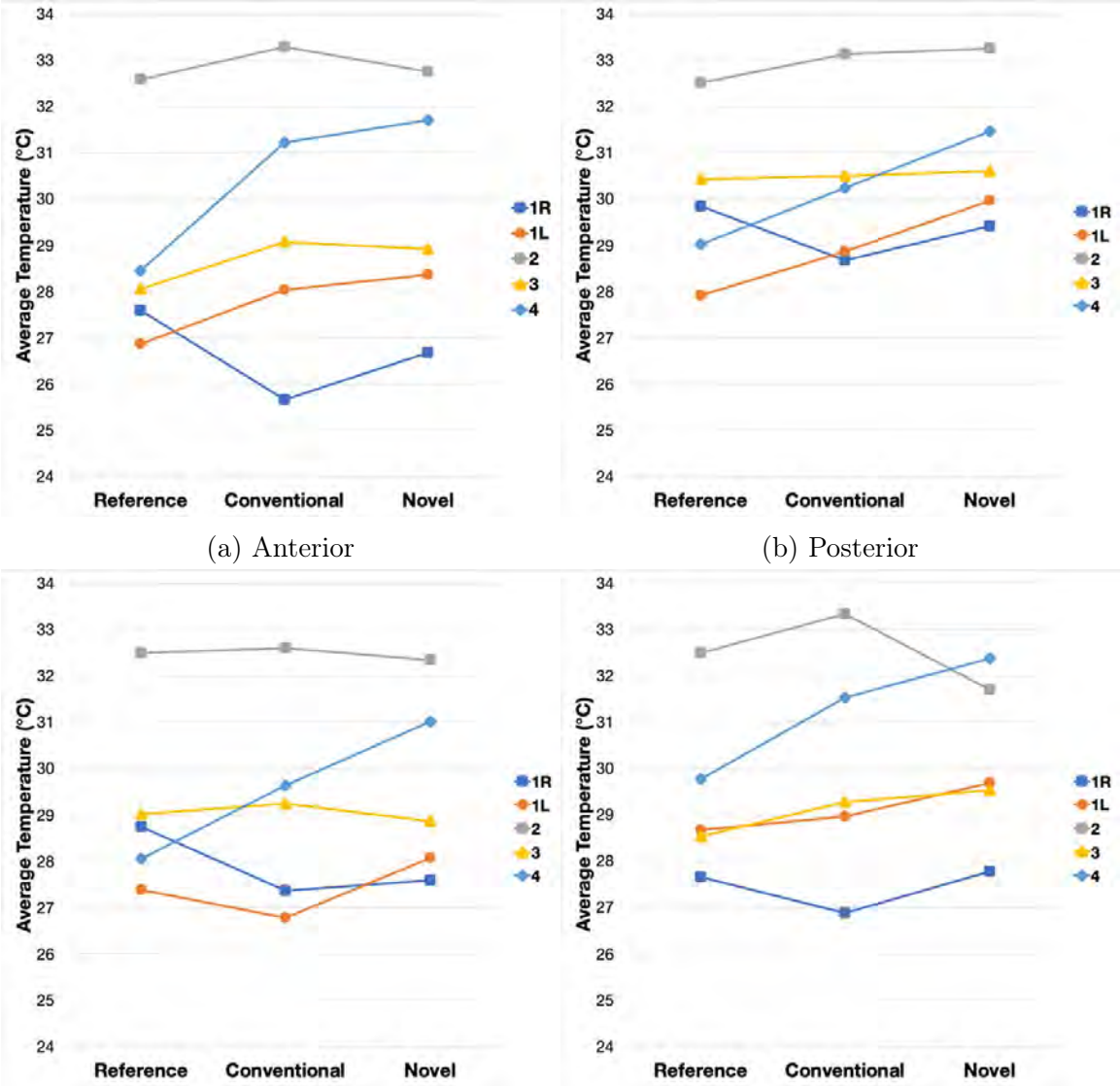

(a) Anterior

(b) Posterior

(c) Medial

(d) Lateral

Figure 3-3 Overall average temperatures for reference, conventional, and novel image sets, separated by location.

Location	P-value	Decision
Anterior	1	Fail to reject null
Posterior	0.55	Fail to reject null
Medial	0.84	Fail to reject null
Lateral	0.69	Fail to reject null
Combined	0.56	Fail to reject null

Table 3.6 P-values and decisions on whether to reject the null hypothesis that there is no statistical difference between conventional and novel datasets. Datasets are percent changes in total average temperature of the residuum immediately post-walking from reference.

residuum. The ROIs are circles of approximately 1 inch diameter. These regions are meant to isolate areas of concern on the residuum. Figure 2-7 shows how the ROIs are positioned for each of the image directions.

The locations that we are most concerned with reducing pain are the distal end and the fibular head regions. The ROI locations are chosen so that location 1 is the distal end for all view directions, and location 4 is approximately at fibular head level for anterior, posterior, and lateral directions. The fibular head cannot be seen from the medial direction.

Tables A.3 and A.4 show a direct comparison percent difference between conventional and novel socket temperatures using Equation 2.4 based on subject and location. Overall the temperature at the distal end is higher after wearing the novel interface versus after wearing the conventional interface. The distal end is a common problematic area for our novel socket design, and during socket fitting and testing it was the most common region of complaint. As described in section 2.1.3, midway through the study a problem with smoothing was found to affect the distal end of the socket. This is corrected in current and future designs, which will help relieve the distal end. Skin temperature at the fibular head level was lower after wearing the novel interface compared to after wearing the conventional from most view angles. The lateral direction gives the best view of the fibular head, and 3 of the subjects showed decrease in temperature from this direction. Anterior and posterior directions are measures of how the temperature effects spread around the residuum, and

reductions in pressure are still seen from these views.

In order to determine the statistical significance of the difference in distal and fibular head between conventional and novel interfaces, percent change from reference for both. Tables A.5 and A.6 show these values for conventional and novel sockets respectively at the distal location. Statistical results using the Mann-Whitney U-test are shown in Table 3.7 and show no significant difference from any of the view directions, as all of the P-values are greater than 0.05. Tables A.7 and A.8 show the percent change from reference for conventional and novel sockets respectively at the fibular head location, and Table 3.8 gives the statistical results. Again this location shows no significant difference in temperature change relative to the reference between conventional and novel sockets based on the P-values.

Location	P-value	Decision
Anterior	0.31	Fail to reject null
Posterior	0.69	Fail to reject null
Medial	0.55	Fail to reject null
Lateral	0.84	Fail to reject null
Combined	0.13	Fail to reject null

Table 3.7 P-values and decisions on whether to reject the null hypothesis that there is no statistical difference between conventional and novel datasets for the distal region of interest.

Location	P-value	Decision
Anterior	0.55	Fail to reject null
Posterior	0.1	Fail to reject null
Medial	0.55	Fail to reject null
Combined	0.71	Fail to reject null

Table 3.8 P-values and decisions on whether to reject the null hypothesis that there is no statistical difference between conventional and novel datasets for the fibular head region of interest.

3.3 Pressure Evaluation

Pressure is measured at 6 locations on the residuum, as shown in Figure 2-8. An example pressure signal is shown in Figure 3-4. The raw signal is cleaned by averaging out any zero values using the immediately adjacent values and then taking a moving average to reduce the effect of noise.

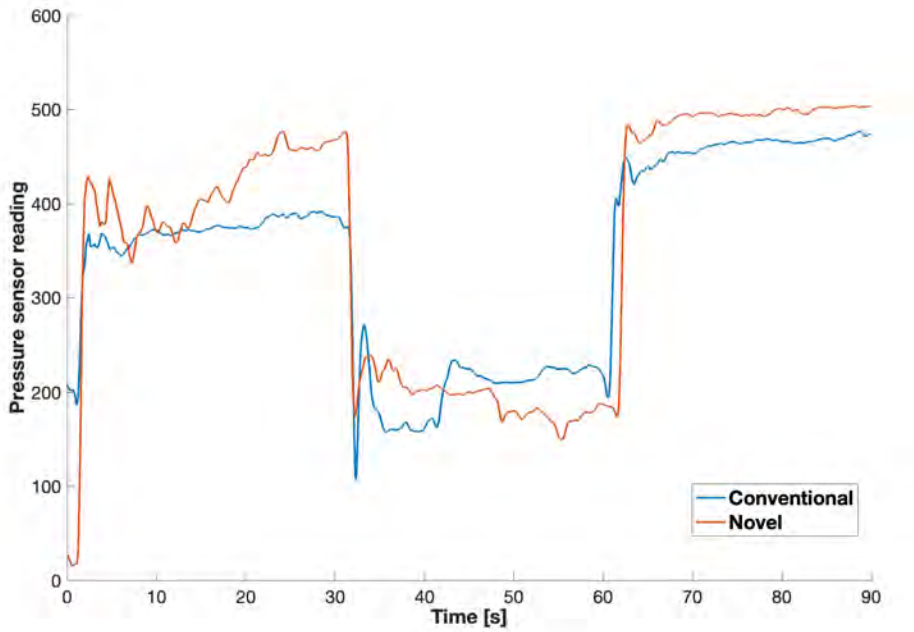

Figure 3-4 An example pressure signal, with zeros cleaned and smoothed using a moving average. The transition from affected single-leg standing to double-leg standing and back to single-leg standing in 30 second intervals is obvious at this location. Subject 1L, patellar tendon.

Due to limitations of the pressure sensor hardware, we are only able to capture the relative pressures within the novel and conventional sockets and thus the absolute values of the pressure signals are unitless. This is why pressures are expressed as a percentage of the maximum value for a given time frame in Figure 3-5.

Figure 3-5 gives the affected-leg only standing normalized pressures relative to the maximum for the conventional and novel sockets at each location.

Relative pressures during the first and last 30s affected leg standing segments are averaged, as we expect the readings to remain relatively consistent after unloading

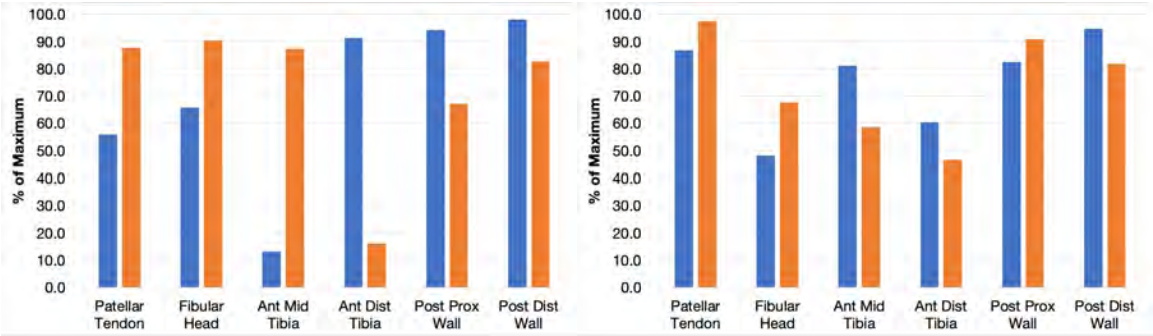

(a) Subject 1R

(b) Subject 1L

(c) Subject 2

(d) Subject 3

(e) Subject 4

Figure 3-5 Relative pressures for affected-leg only standing. The values are averaged over the two affected-leg only trials. Maximum is calculated as the peak pressure reading for the 30-second time period, and the rest of the values are normalized against the maximum. Pressure averages are calculated using a 6-second time window of least variance within the 30s trial.

and reloading. Generally, we are looking to minimize variance in pressure at locations around the socket bar the patellar tendon area. Results using the consistency methodology described in Section 2.2.4 are shown in Table 3.9.

Subject	Conventional ($\%^2$)	Novel ($\%^2$)
1R	1010	757
1L	281	250
2	287	1130
3	740	1360
4	634	336
Average	591	768

Table 3.9 Variances in pressure for conventional and novel sockets by subject, with overall averages.

The results of the Mann-Whitney U-test to compare the variances in pressure between conventional and novel sockets give a P-value of 0.55 which fails to reject the null hypothesis. This means that the variance in pressure between conventional and novel sockets is not significantly different.

Figure B-1 in A shows the double-leg standing normalized pressures for all limbs. During double-leg standing the relative pressures between novel and conventional stayed mostly consistent with affected-leg standing in terms of which socket exerted higher pressure at a specific location. Five locations showed changes in pressure from affected-leg standing: Subject 1R anterior middle tibia, Subject 1R posterior proximal wall, Subject 1R posterior distal wall, Subject 1L patellar tendon,Subject 1L anterior middle tibia, and Subject 4 posterior proximal wall.

Also due to hardware limitations, some signals were lost or too noisy to interpret. These are: Subject 4 Patellar Tendon novel socket signal and Subject 4 Fibular Head. These signals are excluded from the graphed data. Subject 4 is particularly problematic because we found her skin to be unusually conductive, and so if she was touching any grounded metal on accident the readings are unreliable. I attempted to eliminate this by having her use a wooden support while standing, but the problem could not be completely eradicated.

Overall the main locations of concern are the anterior distal tibia and fibular

head locations, and affected-leg standing is more important that double-leg standing because that is when the most load is being applied through the socket. For the anterior distal tibia location, three limbs experienced less pressure in the novel socket. The fibula head location was less successful, with with the novel socket relieving pressure only for Subject 2.

3.4 Questionnaire

The socket evaluation questionnaire gathers direct qualitative feedback from the subjects and is the main source of information about actual feeling and comfort of the novel sockets. The survey gathers general background information on conventional prosthetic interface use and satisfaction and then asks for comparison of the novel system to the conventional. All subjects are relatively to extremely satisfied with their conventional interfaces.

Subject 1 has problems with his conventional socket around his distal tibia end, fibula head, and cutline, but his prosthesis does not generally limit him in daily function. He does have occasional skin irritations due to his socket, and has had laser hair removal on his residual limbs to prevent problems such as ingrown hairs. The socket/liner system is the most limiting aspect of his prosthesis in daily use. He uses a suspension sleeve as his normal form of socket suspension. Subject 1 rates the novel socket highly in all aspects when compared to his conventional socket, for both legs (1R and 1L). Overall he gives the novel sockets much better ratings for fit, slightly better for suspension, and equivalent for ease of donning and doffing. For both legs sitting in the novel and conventional sockets is about the same in terms of pressure and fit. For standing and walking, Subject 1 rates the pressure and fit as much better for both legs. Specifically, the anterior/posterior/medial/lateral edges and walls of the socket are more comfortable, with the knee and distal regions about the same as the conventional socket. There are no regions that cause more discomfort than the conventional socket. The only complaint about the novel sockets is that the cutline around the patellar tendon is slightly too high, which can put pressure on the patella

over time and could lead to injury. Lowering the cutline in this region is a simple fix in our design code.

Subject 2 is very satisfied with his conventional interface, and does not feel it limits his daily activity in any significant way. The most limiting factor of his prosthesis is the foot/ankle system, and this causes him to occasionally avoid slippery or loose terrain and stairs. He is an active runner, so sweat accumulation is also a problem. Overall Subject 2 rates the novel socket a slightly worse fit, and says the socket is about equivalent to the conventional in ease of donning/doffing. He had very low confidence in the suspension system. This is because he is used to a pin-lock on his conventional prosthesis and is unused to a suspension sleeve. This study is not concerned with the suspension mechanism, so this rating does not directly affect the evaluation of the socket. While sitting, the conventional and novel sockets are equivalent to Subject 2, with slightly favorable pressure in the novel. The overall fit of the novel socket was less comfortable while standing and walking, with the subject feeling excessive pressure in the anterior distal region. The other regions of the novel socket are equivalent in feel to the conventional socket. Subject 2 did comment that he feels like the novel socket is at a disadvantage to him because of the suspension system, which he does not feel secure in. While walking he feels his limb move more than in his conventional socket, which could explain the pressure point at the anterior distal tibia.

Subject 3 is also extremely happy with his conventional system. He almost never has skin irritation or pain points, and generally is not limited by his prosthesis. The only activities that he may avoid are lifting heavy objects and doing work outside in hot and humid environments due to sweat accumulation. He also rarely has balancing problems while standing. While his current conventional socket fits well, he says in the past he has had many problems with socket fit, specifically with pain around the fibular head. The fit has been bad enough on previous sockets for him to avoid doing daily activities. Overall Subject 3 gives the novel socket a slightly worse fit with slightly less confidence in socket suspension. His lower confidence in socket suspension is due to the check socket being porous, creating a potential pistoning

problem. While the prosthetist sealed the distal end of the socket during fitting, Subject 3 is still concerned with the suspension. He also says the novel socket is more difficult to put on, but comments that this is mainly due to the difficulty of putting on the silicone liner, so this does not affect the evaluation of socket fit. The novel socket fit was about the same overall for sitting, standing, and walking. The only concerns Subject 3 had were slight pressure on the distal end of his tibia during standing and walking. All other regions of the socket were the same as his conventional socket. In the subject's own words, "overall [he is] impressed with the novel socket ... the socket fit well and was certainly comfortable enough to stand and walk in during testing."

Subject 4 currently has a good conventional interface, but in the past has had poor experiences with different prosthetists and sockets. She has an unusual bone geometry, a sensitive scar on the anterior middle tibia, and a bone spur at the distal tibia end which all make socket fitting a complex task. Her current conventional socket does not usually prevent her from daily activity, and she self-describes herself as a very active person who frequently participates in sports. However, she does avoid using a shower with her prosthesis on and lifting heavy objects. She also sometimes avoids carrying delicate objects and walking on various non-level terrain and stairs. It also does not cause and rashes or sores, but she does have long leg hair so the liner can cause some uncomfortable pulling and she also has a scar line that is easily irritated. She is especially sensitive to socket material and texture to the point where walking in check sockets is more stressful on her limb than walking in a carbon socket of the same geometry because polycarbonate does not flex as naturally as carbon fiber.. Sweat is not a problem for Subject 4, and she says she is actually chronically dehydrated so atrophying over the course of a day is a common problem. The most limiting part of her current prosthesis is the weight and foot/ankle system. Subject 4 gives the novel socket an overall slightly worse fit with similar ease of donning/doffing and similar confidence in the suspension. While sitting and standing the novel and conventional sockets are similar in overall fit and pressure. During standing and walking Subject 4 has a pressure point on the anterior side near the middle of her tibia. She says this is an unusual area for her but could be due to the scar in this region. The novel

socket is equivalent to the conventional socket in all other regions during standing and walking. The subject says that during testing her limb was more swollen than normal due to having just started her period, which led to the socket being more uncomfortable than when she walked in the socket at the prosthetic clinic. She also says that due to her sensitivity to material and texture, standing in the prosthetic with the pressure sensors attached to her limb was especially uncomfortable. The subject says that the socket feels "the shape of the socket is really close", and the main discomfort in comparison to her conventional socket stems from the difference in material.

Chapter 4

Discussion

4.1 Kinematic Results Discussion

With many different gait parameters, it is difficult to evaluate the overall kinematic difference in performance between conventional an novel interfaces. This is why the Mahalanobis distance is used as a combined gain asymmetry metric. The Mahalanobis distance is able to account for multiple different gait metrics and produce singular values that describe how far data is from reference data. None of the subjects have average or maximum Mahalanobis distances greater than the critical value of 7.81 for 3 degrees of freedom. This means that for each subject, no step on the novel system is far enough away from the conventional dataset to be considered a statistically significant outlier. Therefore the kinematic data supports the objective of using this digital method of interface design to create sockets that perform as well as conventional sockets.

The asymmetry data for each metric individually shows changes in symmetry, with many of the metrics moving away from perfect symmetry when switching from novel to conventional systems. This is especially prevalent for the unilateral amputees. However, these changes are not statistically significant when taken together, and the kinematic results cannot be isolated to a specific design flaw. There are many factors that affect gait, and unfamiliarity can play a role in observed gait even if socket fit is good. Most subjects had a maximum of 20 minutes walking on the novel interface

before the kinematic evaluation, while they spend every day on their conventional interfaces. The novel sockets, while aligned and height adjusted by a professional prosthetist, are not specifically designed for the patient's foot-ankle system. The change in liner and socket material and thickness can affect the subject's gait in ways that cannot be isolated from socket design issues specifically. Also, time of day between socket fitting and evaluation can also play a role. Subject 2 was aligned in the early afternoon but his evaluation took place in the evening. His residual limb often atrophies slightly over the course of a day, meaning he will need to add or increase the number of ply socks over his liner to keep socket fit. This slight change in limb volume and geometry can also affect fit and gait.

4.2 Thermal Results Discussion

The thermal results demonstrate a consistent slight increase in residuum temperature from conventional to novel interfaces for subjects 1R, 1L, and 4. Subjects 2 and 3 had more even temperatures between conventional and novel interfaces. with slight decreases in overall temperature from certain view directions. An increase in temperature is not wanted, as it indicates the novel socket is applying more pressure at a region than the conventional socket. However, the greatest increase in temperature is 1.5°C which is equivalent to approximately a 5% increase and is differentiable from noise given the camera's NETD of 0.15°C. It is not clear what the lasting impacts of increased residuum temperature will be over time. However, if the subject does not feel excessive pressure or pain at a region that does experience a temperature increase we are inclined to give more weight to their word. Statistically, there is no difference in total average temperature change from reference when comparing conventional and novel. Statistical tests for all view directions and total combined datasets fail to reject the null hypothesis that there is no statistically significant difference between conventional and novel. This means that the temperature data confirms that the novel interfaces are equivalent in fit to the conventional interfaces from a residuum temperature standpoint.

When looking specifically at the distal and fibular head locations on the residuum, there no significant difference in temperature change from reference between conventional and novel interfaces. This confirms that at these specific locations conventional and novel interfaces are equivalent across all subjects. Direct comparison in temperatures of conventional and novel interfaces indicate that, compared to conventional, the novel interfaces were generally unable to reduce skin temperature at the distal end of the residuum, but did reduce temperature at the fibular head level for 3 of the subjects. The distal end is concerning, as this is the most problematic aspect of the novel interface design based on subject qualitative feedback. Attempts have been made to address this issue as described in Sections 2.1.2 and 2.1.3. We will continue to iterate to improve the distal end comfort in the future.

An interesting result in the thermal data is that some reference temperatures were lower than either the conventional or novel temperatures. As noted in 3.2, this is true for all of Subject 1R's reference measurements. There are several possible explanations for this. The most obvious would be that this is due to the subject's limb not having enough time to cool before taking reference images. However, the subject was given the same amount of time for cooling as other limbs, so I believe this to be unlikely. Subject 1 says that his limbs generally run cold, and this can be seen in the thermal reference images. There is a slight issue with the thermal image processing software used that has difficulty differentiating the limb temperature from the background temperature if the limb is too cold. This can be seen in Figure 4-1 below.

The coldest part of the limb may get partially excluded from the reference image when trying to isolate the limb from the background. Also because Subject 1's limbs generally run cold, the change in average temperature could be attributed to a circulation problem.

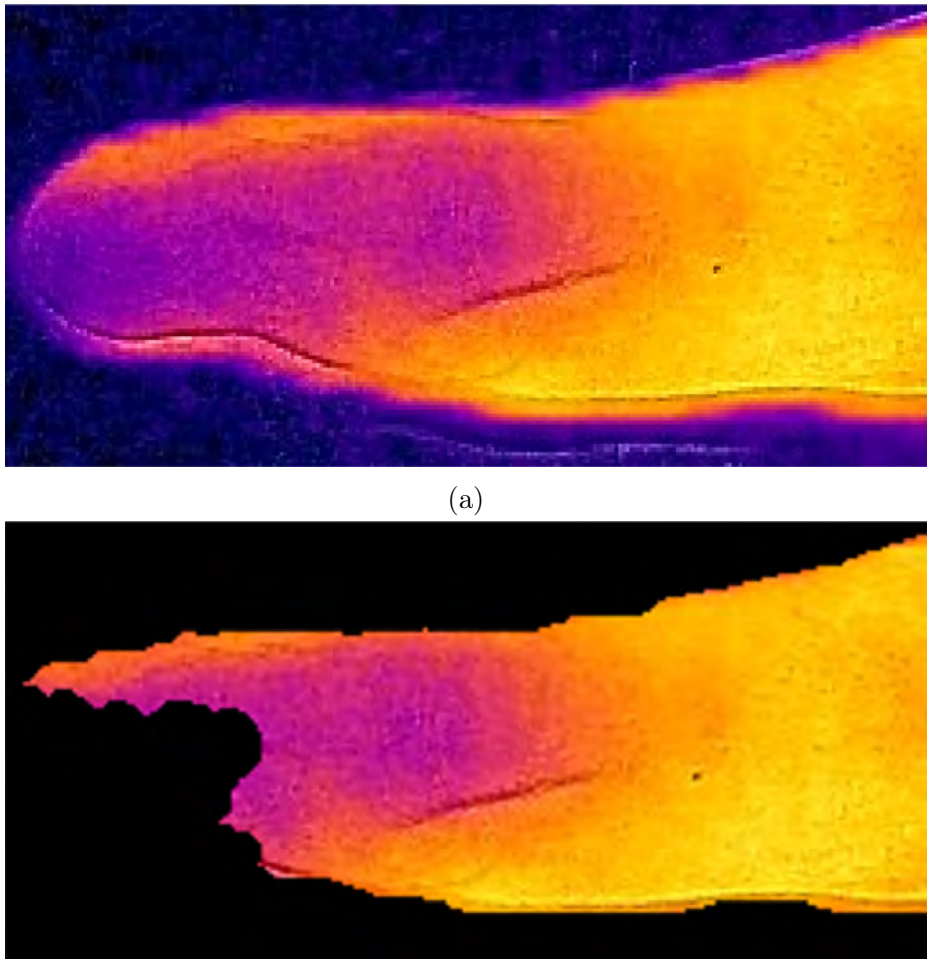

(a)

(b)

Figure 4-1 Figure 4-1a shows the cropped anterior view thermal image for Subject 1R, and Figure 4-1b shows the attempt to isolate the limb from the background. The distal end of the limb is cold and thus difficult to differentiate from the background.

4.3 Pressure Results Discussion

Across the board, pressure during affected-leg only standing is consistent between the first and last 30s periods within each 90s trial in terms of which interface exerted higher pressure at a specific location. This is as expected and validates that the pressure sensors are working in general. The pressure results in general demonstrate a trade-off between reducing pressure at some locations and increasing pressure at others. Changes in geometry to relieve pressure at certain areas may lead to shifts in balance or positioning within the socket, causing increases in pressure at other

locations. For Subjects 1R, 1L, and 3 the novel interface pressure reduction at 3 locations was offset by an increase in pressure at the other 3 locations relative to the conventional. Subject 2 did see a decrease in pressure in the novel interface at 5 of the 6 locations, but Subject 4 saw an increase in pressure for all working sensors. The aim is to achieve more consistent pressure at all locations excluding the patellar tendon. The variance analysis in Table3.9 shows that the average variance accounting for all subjects is lower for the conventional interfaces, but the difference is not statistically significant.

Also interesting to note is the comparison between pressure and thermal results at the anterior distal end and fibular head locations. The thermal results show a slight increase in temperature at the anterior distal end for all patients, while 4 out of 5 limbs actually showed decrease pressure at the distal end. The fibular head location is the opposite, with 3 of 5 limbs showing decrease in temperature with the novel interface while 3 of 4 limbs (Subject 4's fibular head signal failed) show increase in fibular head pressure. This could mean that socket pressure is not the sole cause of increased skin temperature. Other factors that could increase the skin temperature could be liner pressure or friction in the socket from pistoning due to poor suspension, neither of which are measured in this study.

Double-leg standing results led to a reduction in measured pressure on both interfaces, as seen in the 30-60s time period in Figure 3-4. This is expected as load on the affected leg should be halved during this time period. In general, double-leg results were similar to affected-leg results in terms of which interface exerted higher pressures. We do not focus on double-leg results as much as affected-leg results because single-leg affected standing is when the most load is being applied. This means any pressure points will be clearer during affected-leg standing.

Due to the way that the pressure sensors are attached as seen in Figure 2-8, the wires are trapped under the liner and socket. This can lead to discomfort while standing, and sensitivity to this varies by subject. Subjects 1 and 4 felt the most discomfort due to the wires, which can also explain the changes in relative pressure from affected-leg standing and double-leg standing. A less-invasive way to measure

pressure would be necessary to get more accurate results.

4.4 Questionnaire & Qualitative Feedback

Since the aim of this project is to design interfaces that are as comfortable as conventionally made interfaces, patient feedback is important as this is the only way to directly tell what the subject is feeling while wearing the interface. Therefore the questionnaire responses are one of the most important parts of this study. Due to unfamiliarity with socket suspension affecting walking, we give more weight to the sitting and standing comparison Overall, feedback on the fit of the novel socket is positive, and all subjects are enthusiastic about the idea of computational prosthetic interface design. Subject 1 is the only one who rates the fit and pressure of the novel socket as significantly higher, but he also is the least satisfied with the fit of his conventional interface so the modifications allowed by the design algorithm are able to address some of his issues. He does not have any pressure points in the novel sockets, and rates most areas of the socket as more comfortable than his conventional.

The other 3 subjects all have conventional interfaces that fit well with no problems in day-to-day use, so there are few areas the novel interface can improve. These subjects all rate the novel interfaces to be as good as their conventional interfaces while sitting and standing, and only slightly worse while walking. Subjects 2 and 3 feel pressure at the distal end of their tibias in the novel socket and Subject 4 has a pressure point at the anterior middle tibia. None of these points caused pain during the walking trial, but will need to be corrected if the interface is to be used for daily use. Even then, discomfort during walking do not all stem from novel socket fit. Subject 2 especially has concerns with the suspension system, as he is used to a pin-lock rather than a suspension sleeve. He also is not used to walking extensively in the foot/ankle system used in the evaluation, as explained in Section 2.2.2, which might affect the feeling of the socket during walking. Subject 3's fit during walking is also slightly compromised by lack of confidence in the suspension system and the porous nature of the 3D printed socket. Subject 4 is most sensitive to the socket material,

as she much prefers the feel and flex of carbon fiber over the polycarbonate of check sockets. For subjects who are satisfied with their conventional interfaces, results like these are expected and still validate the novel interface design given that the novel socket is still a check socket. Naturally a subject will be more comfortable in the interface they are used to, and the fact that the novel fit for subjects in this study was so close means that computation design is able to get near-optimal geometry while requiring much less time from the patient. All subjects are optimistic about the future of computational interface design. Subject 3 was impressed with how close the novel socket fit was without having to spend much time at the prosthetist. Subjects 3 and 4 have had problems with switching prosthetists and variation in socket fit from one clinic to another in the recent past. They are both excited by the potential of the novel sockets given the fit of the check sockets used in this study. Plaster casting in traditional socket design is particularly uncomfortable for Subject 4, and she likes how the imaging and design in the novel method is less invasive.

4.5 Computational Design Limitations

The limiting factors to the aspects of the computation design pipeline discussed in this study (Demos 7, 8, and 9) are the finite element analysis and the socket fabrication. Based on the size of the residuum and subject weight, FEA for a single socket can take anywhere from 12-36 hours to complete 3 iterations. This also depends somewhat on the processing power of the computer, though comparison between computers was not rigorously tested. Thus computational design can be accelerated by running sockets in parallel on more machines. FEA must be rerun if any changes are made to liner thickness or cutline in Demo 7, or to socket pressure regions in Demo 8. Therefore it can be preferable to make minor design alterations in Demo 9 in order to avoid rerunning FEA. However, the design changes in Demo 9 are less scientifically grounded in residuum geometry and are more artisanal.

The standard lead time on 3D printed check sockets is around a week, including printing and shipping. This can be accelerated to a couple days, with most of the

time cut by using faster shipping methods. Printing of a single socket takes 6-12 hours based on size and thickness. Based on the printing company, multiple sockets can be printed at once and increasing the number of sockets only increases cost but does not increase the printing time significantly. The problems encountered during this study are print failure, where a socket print goes awry and must be reprinted, and total printer failure, where printing capabilities are suspended until repairs can be made. The latter is much worse and happened once during the study.

Accounting for these limitations, a check socket can be designed and delivered in 1-1.5 weeks. Compared to traditional socket design, this presents a more consistent time frame and is less dependent on prosthetist availability, and requires fewer appointments. To maximize the benefits of computational socket design, multiple sockets should be designed and fabricated at once. This will not increase the lead time but will provide the patient with additional options that are not available in traditional socket design.

4.6 Errors

4.6.1 Measurement

The pressure measurement system is the most unreliable of all the devices used, due to its fragile nature and method of attachment. The pressure sensors are taped to the skin, so removing the liner and socket to swap from conventional to novel systems occasionally pulled on the wiring and disconnected a sensor. Also crossed wires or other ways of shorting the circuit were encountered during evaluation and had to be corrected. While these problems are largely avoided in the data included here, I am not sure what happened for Subject 4's fibula head and novel socket patellar tendon signal. These are shown in Figure 4-2 and cannot be distinguished from noise.

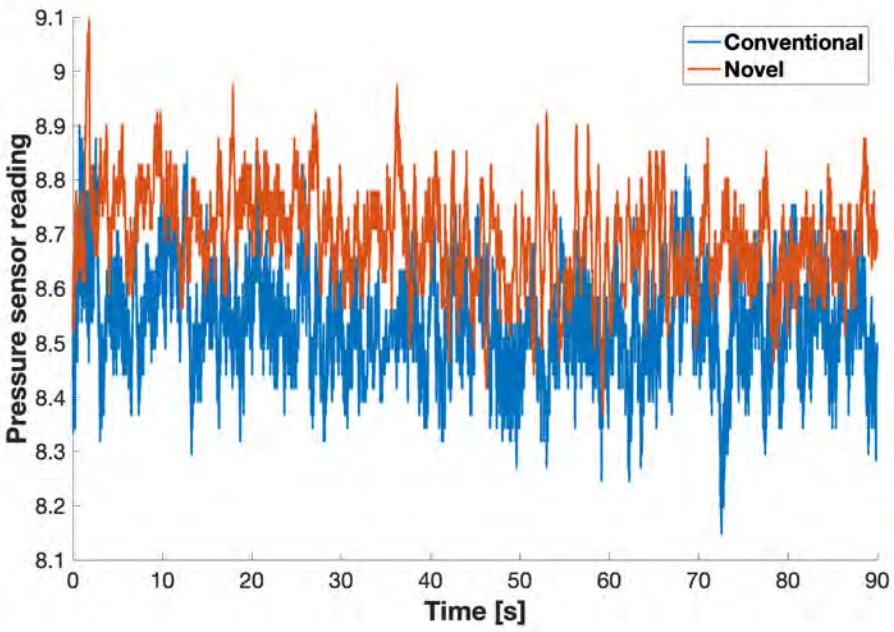

Figure 4-2 Pressure signal for Subject 4's fibular head. Signal is indistinguishable from noise so it is excluded from the results.

4.6.2 Time Between Imaging and Socket Design

An additional problem for this study is due to the Covid-19 pandemic, which put all research studies with patients on hold for a year. The grant that this study is funded by was begun in 2018, and most subjects were imaged in 2019. Most interface design and fitting was done in late 2020 and 2021, which means there was a gap of a year or more between imaging and design. Residual limbs change over time, especially if a person gains or loses weight or changes activity level. Unfortunately changes to these factors were common and accelerated during the pandemic, meaning some image sets were out of date and interfaces, particularly sockets, designed around these old image sets could not achieve good fit. I designed sockets and liners for several patients who were not included in these results due to limb changes. The subjects included maintained relatively consistent weight and activity, and had no other extenuating circumstances in the past two years. Limb changes are also a problem for conventional sockets, and often require a complete redesign. Due to MIT's policies on external visitors during Covid, I was not able to re-image and patients in a reasonable time

frame for the end of this study, which reduced my subject pool. The fact that the novel sockets fit these 5 limbs relatively well on 2+ year old image sets speaks to the design power of the computational algorithm.

4.7 Conclusions

This study evaluated the fit of novel prosthetic interface designs made using a computational framework against traditionally designed interfaces for 4 subjects representing 5 limbs. The results indicate that the novel interfaces do not significantly affect kinematic gait symmetry for all subjects based on a combined gait asymmetry metric using the step time, swing time, and ground reaction force asymmetry comparison. In thermal and pressure metrics, the novel interfaces perform similarly to conventional interfaces and are not significantly different in percent temperature change from reference or pressure consistency. Results vary by subject, but there are no major changes in skin temperature or pressure at any of the locations measured. Qualitative feedback from most of the subjects is positive, and many are surprised at how close the fit of the novel interface is to their conventional interface given the reduced design and testing time. The novel sockets did exhibit some pressure points, but subjects attributed most negative concerns about novel interface fit to unfamiliarity with the suspension system or socket material rather than the socket geometry itself. The subjects were also positive about the future of computational interface design and the benefits it can bring over traditional socket design, such as elimination of plaster casting, reduced reliance on prosthetist skill, and custom liners. This study is part of an ongoing broader project to computationally design interfaces using both MRI and CT image sets for patients in the United States and Mexico, and the results analyzed here are a promising indicator of the progress of this design method.

4.8 Thesis Contributions

This thesis outlines a novel prosthetic interface design method that uses MRI imaging to extract transtibial residual limb geometry to computationally design prosthetic sockets and liners. Socket geometry is determined by assigning variable pressure to regions on the limb based on bone location and geometry, and then running finite element analysis to simulate loading conditions to optimize the socket fit. The evaluation of novel interfaces designed in this manner indicates that the interfaces are comparable to traditionally designed interfaces that subjects wear daily. The benefits of this method include lower overall cost and reduced time for new interfaces, precise manipulation of interface geometry, and retaining of patient-specific preferences for future designs. Improvement of this computational algorithm has the potential to reduce the time and cost associated with making a quality prosthetic interface. As the interface often determines the usability of the entire prosthesis, this will improve mobility and health for those without comfortable interfaces.

4.9 Future Work

The logical next step in this work is to use the novel computationally-designed geometry to create carbon fiber sockets and have patients use them for extended periods of time. The longer adjustment period and better material will reduce confounding factors such as suspension unfamiliarity, weight differences, and material sensitivity. This will allow evaluation of the long-term comfort and success of the novel design method.

Design changes to the socket in Demos 7, 8, and 9 are mostly made via patient feedback and thus require at least one fitting to determine patient preferences, sensitive areas on the residuum, and pain points. Default pressures of 0x/3.0x/1.0x, 0x/3.2x/1.2x, and 0x/3.4x/1.4x are based on previous subjects and found to generally work for initial fittings, but often need to be changed to improve fit. To improve the accuracy of initial fit, I hope to use soft tissue depth to help determine the best

starting pressures for new subjects. I hypothesize that limbs with increased soft tissue depth should require lower socket fitting pressures.

Our current design does not take into account soft tissue material properties, which can affect interface fit in addition to bone and skin geometry. The Biomechatronics group has unused soft tissue material data for several subjects obtained through palpation studies. This data should be able to provide highly accurate soft tissue properties compared to previous indentation data. I would like to revisit multi-material sockets to apply this data to socket design to locally vary socket compliance in addition to optimizing the socket geometry. Improvements in additive manufacturing processes in recent years will allow fabrication of multi-material sockets that hopefully avoid the problems described in Section 1.2.

In order to validate the finite element analysis model for socket pressure, there needs to be a way to validate absolute pressure values while a subject stands in a socket. This requires a more accurate load sensing mechanism than force sensing resistors, and many precision load cells are too large to attach inside the socket. One method that has been attempted is mounting load cells to the outside of a custom socket so that the load cell head is flush against the inside of the socket. Another possible way is creating specialized liners that incorporate pressure sensing devices within the liner. There are two interesting paths forward that I have seen for this. The first involves using newly-developed strain-sensing filaments that detect deformation and can be encased in a silicone liner [30, 31]. Since pressure causes local deformation, these filaments could be used to measure pressure depending on their accuracy. The second method also involves using deformation to measure pressure. Benjamin Miller and Mathias Kolle's Lab for Biologically Inspired Photonic Engineering at MIT have created a process to coat surfaces with a film that changes color based on deformation. This coating has tunable properties and can adhere to many different materials. A liner could be coated and used in a socket, and the color map can be correlated to pressure levels.

A main goal of computational prosthetic interface design is to provide comfortable interfaces to people in regions of the world that do not have access to affordable or ad-

equate prosthetic care. The aim is to create a prosthetic mobile clinic that can access regions with large populations of amputees and provide imaging, consultation, and treatment. A portable CT system will facilitate imaging in the field, expanding access to those unable to travel to a clinic and those in hard-to-reach areas. Cloud-based computing enables the remote design of interfaces, reducing the clinical workload of caregivers and time required from the patient. This will allow more patients to be seen, which is crucial among populations with high rates of amputation. Low-cost manufacturing also makes it feasible to replace sockets at more frequent intervals, improving the long-term health and comfort of patients. This computational design framework aims to eliminate the variation based on prosthetist skill of socket quality and fit , as everyone will get high-quality personalized care. Successful implementation of computational prosthetic interface design in mobile prosthetic clinics will help democratize prosthetic care and facilitate major improvements quality of life for persons living with amputation.

Appendix A

Additional Tables

Subject	Anterior (%)	Posterior (%)	Medial (%)	Lateral (%)
1R	-7.0	-3.9	-4.8	-2.8
1L	4.3	3.4	-2.2	0.99
2	2.2	1.9	0.35	2.6
3	3.7	0.22	0.77	2.6
4	9.8	4.2	5.7	5.9

Table A.1 Percent change from reference for conventional socket, using Equation 2.3.

Subject	Anterior (%)	Posterior (%)	Medial (%)	Lateral (%)
1R	-3.3	-1.4	-4.0	0.41
1L	5.6	7.3	2.5	3.5
2	0.53	2.3	-0.47	-2.5
3	3.1	0.54	-0.54	3.5
4	11	8.5	10	8.8

Table A.2 Percent change from reference for novel socket, using Equation 2.3.

Subject	Anterior % Difference	Posterior % Difference	Medial % Difference	Lateral % Difference
1R	7.8	1.4	5.0	2.0
1L	0.4	3.4	9.7	6.8
2	1.8	0.32	2.5	-3.7
3	2.4	-0.35	-0.67	1.1
4	4.2	15	7.8	-1.3

Table A.3 Percent difference in temperature between the novel and conventional sockets at the distal end of the residuum. A negative value means a lower temperature on the novel socket.

Subject	Anterior % Difference	Posterior % Difference	Lateral % Difference
1R	6.4	6.1	5.2
1L	-3.9	3.0	-3.0
2	-3.0	-2.0	-1.8
3	-4.0	-3.1	-6.0
4	-0.30	3.9	2.7

Table A.4 Percent difference in temperature between the novel and conventional sockets at the fibular head level of the residuum. A negative value means a lower temperature on the novel socket.

Subject	Anterior (%)	Posterior (%)	Medial (%)	Lateral (%)
1R	-3.2	4.1	-11	-3.7
1L	5.5	13	-4.0	2.1
2	2.1	2.7	-2.8	-2.5
3	7.1	0.62	8.8	3.2
4	7.9	6.2	6.5	13

Table A.5 Percent change from reference for novel socket at the distal region of interest.

Subject	Anterior (%)	Posterior (%)	Medial (%)	Lateral (%)
1R	6.6	5.5	-6.4	-2.0
1L	5.9	18	5.9	9.1
2	3.8	2.9	-0.24	-6.2
3	9.9	0.20	8.1	4.2
4	12	24	15	12

Table A.6 Percent change from reference for novel socket at the distal region of interest.

Subject	Anterior (%)	Posterior (%)	Lateral (%)
1R	-6.8	-6.9	-8.6
1L	12	-2.9	9.3
2	6.8	1.9	6.0
3	5.1	3.2	9.1
4	11	2.9	5.4

Table A.7 Percent change from reference for conventional socket at the fibular head region of interest.

Subject	Anterior (%)	Posterior (%)	Lateral (%)
1R	-0.6	-1.0	-3.5
1L	7.5	-0.16	6.1
2	3.7	-0.12	4.3
3	0.84	0.33	3.1
4	10	6.9	8.3

Table A.8 Percent change from reference for novel socket at the fibular head region of interest.

Appendix B

Additional Figures

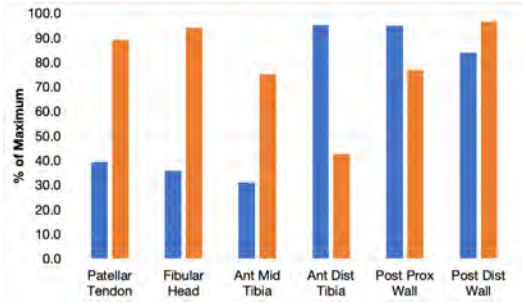

(a) Subject 1R

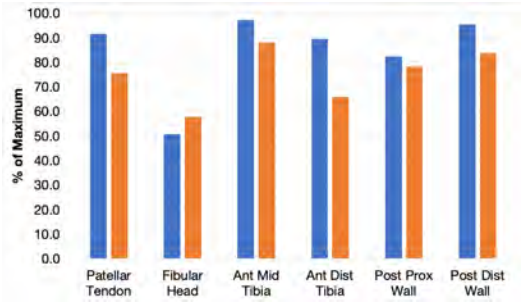

(b) Subject 1L

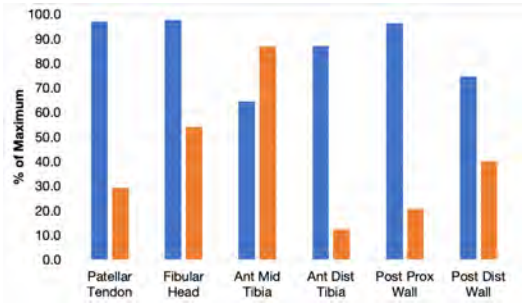

(c) Subject 2

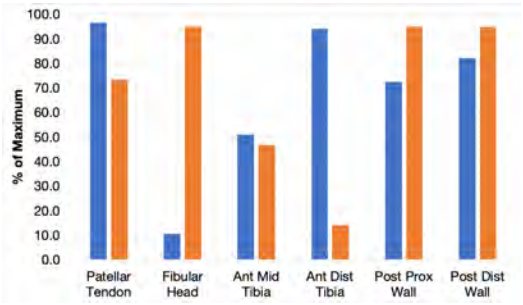

(d) Subject 3

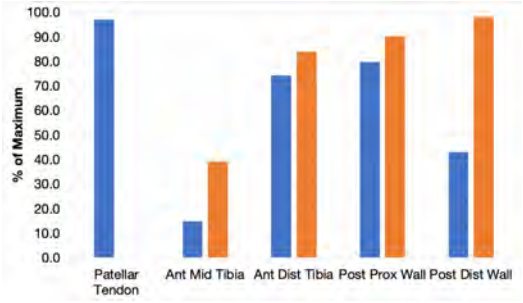

(e) Subject 4

Figure B-1 Relative pressures for double-leg standing. Method of calculating relative pressures is the same as for affected-leg only standing.

Bibliography

[1] Kathryn Ziegler-Graham et al.
"Estimating the Prevalence of Limb Loss in the United States: 2005 to 2050".
In: *Archives of Physical Medicine and Rehabilitation* 89.3 (Mar. 2008),
pp. 422–429. ISSN: 00039993. DOI: 10.1016/j.apmr.2007.11.005.

[2] *Amputee Statistics You Ought to Know*. Tech. rep. 2012. URL:
https://advancedamputees.com/amputee-statistics-you-ought-know.

[3] "Limb Loss Statistics - Amputee Coalition". In: (). URL: https:
//www.amputee-coalition.org/resources/limb-loss-statistics/.

[4] Aisha Lofters et al.
"Patients living with disabilities: The need for high-quality primary care."
In: *Canadian family physician Medecin de famille canadien* 62.8 (Aug. 2016),
pp. 457–64. ISSN: 1715-5258.

[5] Amene Sabzi Sarvestani and Afshin Taheri Azam.
"Amputation: a ten-year survey."
In: *Trauma monthly* 18.3 (Dec. 2013), pp. 126–129. ISSN: 2251-7464.
DOI: 10.5812/traumamon.11693.

[6] Jacob C. Seidell.
"Obesity, insulin resistance and diabetes — a worldwide epidemic".
In: *British Journal of Nutrition* 83.S1 (June 2000), S5–S8. ISSN: 0007-1145.
DOI: 10.1017/S000711450000088X.

[7] Linda S. Geiss et al.
"Resurgence of Diabetes-Related Nontraumatic Lower-Extremity Amputation in the Young and Middle-Aged Adult U.S. Population".
In: *Diabetes Care* 42.1 (Jan. 2019), pp. 50–54. ISSN: 0149-5992.
DOI: 10.2337/dc18-1380.

[8] M W Legro et al. "Issues of importance reported by persons with lower limb amputations and prostheses." In: *Journal of rehabilitation research and development* 36.3 (July 1999), pp. 155–63. ISSN: 0748-7711.

[9] David Moinina Sengeh and Hugh Herr.
"A Variable-Impedance Prosthetic Socket for a Transtibial Amputee Designed from Magnetic Resonance Imaging Data".
In: *JPO Journal of Prosthetics and Orthotics* 25.3 (July 2013), pp. 129–137.
ISSN: 1040-8800. DOI: 10.1097/JPO.0b013e31829be19c.

[10] *How to Make Prosthetics*. Tech. rep. URL:
https://www.scheckandsiress.com/blog/how-to-make-prosthetics/.

[11] M. Spittle, R. J. Collins, and H. Conner.
"The incidence of pressure sores following lower limb amputations".
In: *Practical Diabetes International* 18.2 (Jan. 2001), pp. 57–61.
ISSN: 13578170. DOI: 10.1002/pdi.139.

[12] Heikki Uustal.
"Prosthetic Rehabilitation Issues in the Diabetic and Dysvascular Amputee".
In: *Physical Medicine and Rehabilitation Clinics of North America* 20.4 (Nov. 2009), pp. 689–703. ISSN: 10479651. DOI: 10.1016/j.pmr.2009.06.014.

[13] David M. Sengeh et al. "Multi-material 3-D viscoelastic model of a transtibial residuum from in-vivo indentation and MRI data". In: *Journal of the Mechanical Behavior of Biomedical Materials* 59 (June 2016), pp. 379–392.
ISSN: 17516161. DOI: 10.1016/j.jmbbm.2016.02.020.

[14] *The PandoFit Solution*. URL: https://prosfit.com/solution.

[15] Kevin M. Moerman et al. “Automated and Data-driven Computational Design of Patient-Specific Biomechanical Interfaces”. 2016. DOI: https://doi.org/10.31224/osf.io/g8h9n.

[16] Kevin M Moerman. “GIBBON: The Geometry and Image-Based Bioengineering add-On”. In: *The Journal of Open Source Software* 3.22 (Feb. 2018), p. 506. DOI: 10.21105/joss.00506.

[17] Dana Solav et al. “MultiDIC: An Open-Source Toolbox for Multi-View 3D Digital Image Correlation”. In: *IEEE Access* 6 (2018), pp. 30520–30535. ISSN: 2169-3536. DOI: 10.1109/ACCESS.2018.2843725.

[18] Dana Solav et al. “A Framework for Measuring the Time-Varying Shape and Full-Field Deformation of Residual Limbs Using 3-D Digital Image Correlation”. In: *IEEE Transactions on Biomedical Engineering* 66.10 (Oct. 2019), pp. 2740–2752. DOI: https://doi.org/10.1109/TBME.2019.2895283.

[19] Ming Zhang and Winson C. C. Lee. “Quantifying the Regional Load-Bearing Ability of Trans-Tibial Stumps”. In: *Prosthetics & Orthotics International* 30.1 (Apr. 2006), pp. 25–34. ISSN: 0309-3646. DOI: 10.1080/03093640500468074.

[20] Steve A. Maas et al. “FEBio: Finite elements for biomechanics”. In: *Journal of Biomechanical Engineering* 134.1 (2012). ISSN: 01480731. DOI: 10.1115/1.4005694.

[21] G. Taubin. “Curve and surface smoothing without shrinkage”. In: *Proceedings of IEEE International Conference on Computer Vision*. IEEE Comput. Soc. Press, pp. 852–857. ISBN: 0-8186-7042-8. DOI: 10.1109/ICCV.1995.466848.

[22] *Essentium PCTG Technical Data Sheet*. URL: https://www.essentium.com/wp-content/uploads/2020/08/TDS-Essentium-PCTG_v1.0-Minus-3D.pdf.

[23] Arezoo Eshraghi et al. “Pistoning assessment in lower limb prosthetic sockets”. In: *Prosthetics & Orthotics International* 36.1 (Mar. 2012), pp. 15–24. ISSN: 0309-3646. DOI: 10.1177/0309364611431625.

[24] Tyagi Ramakrishnan, Seok Hun Kim, and Kyle B. Reed. “Human Gait Analysis Metric for Gait Retraining”. In: *Applied Bionics and Biomechanics* 2019 (Nov. 2019), pp. 1–8. ISSN: 1176-2322. DOI: 10.1155/2019/1286864.

[25] Tyagi Ramakrishnan, Haris Muratagic, and Kyle B. Reed. “Combined gait asymmetry metric”. In: *Proceedings of the Annual International Conference of the IEEE Engineering in Medicine and Biology Society, EMBS*. Vol. 2016-October. Institute of Electrical and Electronics Engineers Inc., Oct. 2016, pp. 2165–2168. ISBN: 9781457702204. DOI: 10.1109/EMBC.2016.7591158.

[26] Stephen Sprigle et al. “Clinical Skin Temperature Measurement to Predict Incipient Pressure Ulcers”. In: *Advances in Skin & Wound Care* 14.3 (May 2001), pp. 133–137. ISSN: 1527-7941. DOI: 10.1097/00129334-200105000-00010.

[27] H. B. Mann and D. R. Whitney. “On a Test of Whether one of Two Random Variables is Stochastically Larger than the Other”. In: *The Annals of Mathematical Statistics* 18.1 (Mar. 1947), pp. 50–60. ISSN: 0003-4851. DOI: 10.1214/aoms/1177730491.

[28] M W Legro et al. “Prosthesis evaluation questionnaire for persons with lower limb amputations: assessing prosthesis-related quality of life.” In: *Archives of physical medicine and rehabilitation* 79.8 (Aug. 1998), pp. 931–8. ISSN: 0003-9993. DOI: 10.1016/s0003-9993(98)90090-9.

[29] “Critical Values of the Chi-Square Distribution”. In: *NIST/SEMATECH e-Handbook of Statistical Methods*. NIST/SEMATECH, 2013. Chap. 1.3.6.7.4.

DOI: https://doi.org/10.18434/M32189. URL: https://www.itl.nist.gov/div898/handbook/eda/section3/eda3674.htm.

[30] Gabriel Loke et al. "Recent Progress and Perspectives of Thermally Drawn Multimaterial Fiber Electronics".
In: *Advanced Materials* 32.1 (Jan. 2020), p. 1904911. ISSN: 0935-9648. DOI: 10.1002/adma.201904911.

[31] Yujing Zhang et al. "Thermally Drawn Stretchable Electrical and Optical Fiber Sensors for Multimodal Extreme Deformation Sensing".
In: *Advanced Optical Materials* 9.6 (Mar. 2021), p. 2001815. ISSN: 2195-1071. DOI: 10.1002/adom.202001815.